Using naturalistic and driving simulator data to model driver responses to unintentional lane departures

Transportation Research Part F: Psychology and Behaviour 100 (2024) 361–387

Contents lists available at ScienceDirect

Transportation Research Part F: Psychology and Behaviour

journal homepage: www.elsevier.com/locate/trf

Using naturalistic and driving simulator data to model driver responses to unintentional lane departures

Malin Svärd [a,*], Gustav Markkula [b], Mikael Ljung Aust [c], Jonas Bärgman [a]

[a] Division of Vehicle Safety, Department of Applied Mechanics, Chalmers University of Technology, Gothenburg, Sweden
[b] Institute for Transport Studies, University of Leeds, Leeds, United Kingdom
[c] Volvo Cars Safety Centre, Gothenburg, Sweden

ARTICLE INFO

Keywords:
Driver model
Lane departure
Intermittent control
Safety benefit
Steering

ABSTRACT

Unintentional lane departures on straight roads cause many road fatalities each year. The objective of this study was to explore and model drivers' recovery steering maneuvers in unintentional drift situations, to enable the prospective safety benefit assessment of lane departure warning and avoidance systems through counterfactual simulations. The timing and amplitude of the steering adjustments drivers make to avoid lane departure were studied over three data sets with different origins, consisting of both naturalistic data and experimental data from a driving simulator study. With respect to timing, the main finding was that visually distracted drivers often initiate the corrective steering response prior to looking back towards the road, demonstrating that lane-keeping information in the visual periphery is sufficient to trigger the response. As for steering amplitude, the observed amplitudes were correlated against different lane departure risk metrics from the literature, resulting in a model capable of accounting for human behavior across all three data sets with good performance. Surprisingly, a very simple model (which describes the steering amplitude as increasing quadratically with the vehicle's orientation to the road) predicted the amplitude of the primary corrective steering adjustment better than models based on more complex lane departure risk metrics. This result indicates that drivers scale the amplitude of their steering adjustment to the steering input needed to get the vehicle back in the lane already at first response. However, it was possible to obtain a similar model fit using a more complex threshold model, with different dynamics depending on the vehicle's current orientation to the road. We discuss how these findings can be applied to models of human steering for safety benefit assessment.

1. Introduction

Unintentional lane departures contribute to a large portion of road fatalities on European and US roads (Kuehn et al., 2009; Kusano & Gabler, 2014; Najm et al., 2007; Strandroth, 2015). In fact, studies show that as many as one-third of all road fatalities can be attributed to lane departures (Kusano & Gabler, 2014; Strandroth, 2015). Driver distraction and inattention degrade lane-keeping performance (Horrey et al., 2008; Kountouriotis & Merat, 2016; Okafuji et al., 2018; Reed-Jones et al., 2008) and have been

* Corresponding author at: Division of Vehicle Safety, Department of Applied Mechanics, Chalmers University of Technology, Volvo Cars Safety Centre, Volvo Car Corporation, Volvo Cars Safety Centre, 418 78 Gothenburg, Sweden.
E-mail addresses: malin.svard@chalmers.se (M. Svärd), G.Markkula@leeds.ac.uk (G. Markkula), Mikael.ljung.aust@volvocars.com (M. Ljung Aust), jonas.bargman@chalmers.se (J. Bärgman).

https://doi.org/10.1016/j.trf.2023.11.021
Received 30 April 2023; Received in revised form 27 October 2023; Accepted 30 November 2023
Available online 19 December 2023

identified as the leading causes of roadway departures (Amarasingha & Dissanayake, 2014; McLaughlin et al., 2009; Najm et al., 2007), with the majority of the incidents occurring on straight roads (McLaughlin et al., 2009; Sternlund, 2017).

Several advanced driver assistance systems (ADAS) targeting lane departures caused by visual distraction have emerged in recent years. The traffic safety benefit of these systems, such as Lane Departure Warning (LDW) and Lane Keeping Assistant Systems (LKAS), has been estimated using real-world data based on insurance claims and in-depth studies (Isaksson-Hellman & Lindman, 2018; Utriainen et al., 2020). Counterfactual simulations in a virtual environment could complement these retrospective studies (which examine crashes that have already happened) with a prospective benefit assessment (which estimates the benefit of potential systems), while also having the capacity to provide a large amount of data at a relatively low cost (see, e.g., Alvarez et al., 2017; International Organization for Standardization, 2019; Page et al., 2015). However, counterfactual simulations require that a computational driver model featuring realistic human steering behavior be in the loop.

Human steering behavior has been extensively studied, and several models targeting drivers' lane-keeping behavior have been proposed (Donges, 1978; Goodridge et al., 2022; Land & Horwood, 1995; Markkula et al., 2018; Okafuji et al., 2018; Salvucci & Gray, 2004; Summala et al., 1996; Wilkie & Wann, 2003). It has been suggested that the driver uses two levels of control: compensatory and anticipatory (Donges, 1978). The compensatory level uses information from regions near the vehicle, such as lane position, to stabilize the vehicle in the lane—while the anticipatory level uses information from far regions, such as optic flow, to guide steering along a desired path (Mole et al., 2016; Okafuji et al., 2018; Salvucci & Gray, 2004). A common way to model anticipatory control is through aim point models (Donges, 1978; Kondo & Ajimine, 1968; Mole et al., 2016; Salvucci & Gray, 2004; Zhou et al., 2020), which build upon the assumption that drivers steer by looking ahead and using one or several aim points along the future path. The aim points constantly move along with the vehicle: the relative distance from the aim point to the vehicle is kept constant. However, more recent literature suggests that, alternatively, drivers use target waypoints along the predicted future path to steer during routine driving (Lappi et al., 2020; Tuhkanen et al., 2019). In contrast to aim points, target waypoints have fixed locations (thus, they do not move with the vehicle), and drivers shift their gaze to a new waypoint at regular intervals. In either case, driver behavior during everyday driving does not necessarily generalize to recovery steering in critical lane departure situations. Markkula (2015) suggested that everyday driving can be modeled with closed-loop control. However, he added that evasive maneuvers are often performed with a single ballistic adjustment in response to the critical scenario, motivating an open-loop control model.

Recent research has indicated that driver motor control consists of intermittent actions. Several computational driver models have been based on this finding (Cheng et al., 2020; Gordon & Srinivasan, 2014; Markkula et al., 2018; Martínez-García et al., 2016; Martínez-García & Gordon, 2017, 2018; Svärd et al., 2017). Martínez-García and Gordon (2017, 2019) designed a multiplicative human control (MHC) model for lane keeping, motivated by previous research showing that human control responses in compensatory tasks can be characterized by a multiplicative controller (i.e., each control action depends on the product of all previous control errors). In their proposed model, the driver steers intermittently based on information from both the compensatory and anticipatory levels. For compensatory control, the model uses the change in splay angle error. The splay angle is the optical projection of the angle between a vertical line and the lane markers on either side of the road (Beall & Loomis, 19; E. S. Calvert, 1954; L. Li & Chen, 2010; Warren, 1982; see Section 2.3.2). The splay angle error is defined as the difference between the left and right splay angle and provides information about the vehicle's lateral position in the lane, independent of the yaw rotation. Anticipatory control is modeled by calculating the critical normalized yaw rate (CNYR), a yaw rate-based measure that can be used to indicate whether the vehicle will exceed the lane boundaries within a certain preview time. A value between −1 and 1 corresponds to the vehicle staying in-lane. Cheng et al. (2020) also assumed intermittent steering actions and showed how inverse time-to-lane-crossing (iTLC) can be used to predict driver steering interventions (a higher value indicates a higher risk of lane departure). Cheng and colleagues proposed that the driver follows a satisficing behavior, with a distinct peak in the probability of a steering correction around a specific iTLC value. Little has been done to computationally model driver steering in lane departure situations, with the rare exception of models based on a non-cognitive framework (e.g., artificial neural networks or nonlinear autoregressive models with exogenous input) whose purpose was to make the lane departure recovery maneuver of LKAS less intrusive (Zulkepli et al., 2018). Most literature on driver steering behavior targets non-critical situations on curved roads (e.g., A. Li et al., 2019; Markkula et al., 2018; Salvucci, 2006; Salvucci & Gray, 2004; Zhou et al., 2020), during lane changes (e.g., Cheng et al., 2020; Salvucci, 2006; Salvucci & Gray, 2004), or during routine lane keeping (Gordon et al., 2009; Gordon & Srinivasan, 2014; Markkula et al., 2018; Martínez-García & Gordon, 2017, 2018; Salvucci, 2006; Salvucci & Gray, 2004). To the authors' best knowledge, none of these models take the driver's gaze direction into consideration. Though a few studies have analyzed lane departure recovery maneuvers (Eriksson et al., 2018; Hildreth et al., 2000; Navarro et al., 2017), no models of drivers' steering timing and amplitude have been suggested outside of the routine lane-keeping domain. Goodridge et al. (2022) proposed that the timing and amplitude of human steering responses when exposed to a set of lane departure variations (defined by the starting position and heading angle) could accurately be explained by the accumulation over time of perceptual evidence about steering, but the authors did not specify a model to describe the mechanisms in more detail. A similar setup was used in a driving simulator study by Hildreth et al. (2000). They demonstrated that larger departure angles result in increased steering correction magnitudes. Later, the two-point steering model by Salvucci & Gray (2004) was able to accurately replicate the steering profiles of two selected drivers from Hildreth's study. However, the model explicitly assumes that the driver aims to reposition the vehicle in the center of the lane, which may not always be the case (not least due to differences between drivers). Moreover, the model parameters were individually tuned to each driver.

The overall aim of the current work is to explore and model recovery maneuvers in unintentional lane departures from straight roads caused by drift (i.e., not traction loss). To achieve this aim, three data sets were used to analyze the timing and amplitude of the primary corrective steering adjustment, defined as the first steering adjustment in the opposite direction of the lane departure (i.e., the driver's first corrective steering action). Since many lane departures without prior traction loss are caused by visual distractions

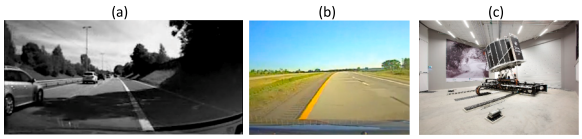

Fig. 1. Illustrations of the three data sets used in this study. *Panel a:* Forward view from a lane departure event in the EyesOnRoad data set. *Panel b*: Forward view from a lane departure event in the SHRP2 data set. *Panel c*: Outward view of the driving simulator used in the Run-off-road simulator study data set. Photo credit: Hejdlösa bilder / VTI.

Table 1
An overview of the most important data set differences.

Data set	Source (country)	Gaze data source	Departure types	No. of departures
EyesOnRoad	Naturalistic (Sweden)	Manual annotation	Naturally occurring lane exceedances without crashes	34
SHRP2	Naturalistic (US)	Manual annotation	Naturally occurring lane exceedances leading to a near-crash or crash	6
Run-off-road simulator study	Driving simulator (Sweden)	Eye tracker	Artificially induced events with high risk of lane exceedance	12

(Sternlund, 2017), one objective is to describe the timing of the primary corrective steering adjustment in relation to the driver's last off-road glance. A second objective is to identify metrics associated with the driver's subjectively perceived lane departure risk. The third and final objective is to use the identified lane departure risk metrics as predictors in models of the primary corrective adjustment's steering amplitude.

2. Method

The analysis in this paper was performed using data from three different sources, to make the potential driver model as generally valid as possible. This section gives an overview of the data sets and describes how lane departure events were extracted from each. Moreover, descriptions of the data preprocessing required for each data set are provided, as are details on how to identify the primary corrective steering adjustment for each lane departure event.

2.1. Data

Two of the data sets comprised naturalistic driving data collected in real cars on real roads. The first data set (referred to here as "the EyesOnRoad data set"; see Section 2.1.1) consisted of relatively shallow angle lane departures which the drivers were able to resolve efficiently, while the second ("the SHRP2 data set"; see Section 2.1.2) contained lane departure crashes and near-crashes.

Relevant lane departure events were identified by database queries, followed by manual vid***eo inspection to ensure that only *unintentional drift events* with a minimal number of confounding factors were included. Drivers can be assumed to adopt a satisficing lane-keeping behavior (Boer, 2016; Summala, 2007) and, thus, accept some lateral drift within their personal comfort boundaries. However, once the boundaries are exceeded, the following departure can be considered unintentional. In practice, events were considered potentially intentional, and were consequently excluded, if they were influenced by infrastructure (e.g., intersections or construction sites), environment (e.g., glare), or other road participants (e.g., oncoming heavy traffic in the adjacent lane). Events known to involve driver intoxication or excessive speeding were also excluded, although this information was not available for all events. The minimum departure speed was set to 50 km/h to avoid events in places with an abundance of confounding factors, such as urban intersections or parking lots. Examples of the forward views at the departure in the naturalistic data sets are provided in Fig. 1 (Panels a and b).

Since the number of highly critical lane departures was relatively low in the naturalistic data sets, these events were complemented with a third data set collected in a driving simulator study using a high-fidelity full-motion simulator ("the Run-off-road simulator study data set"; see Section 2.1.3). The lane departures in the simulator study were artificially induced (i.e., vehicle rotation without kinematic cues while the driver was looking away) and had larger relative yaw angles than were observed in the other data sets. Fig. 1 (Panel c) shows the outward view of the driving simulator used to collect the Run-off-road simulator study data set. Furthermore, Table 1 highlights the most important data set differences.

2.1.1. The EyesOnRoad data set

The EyesOnRoad data set (Karlsson et al., 2016) consists of Swedish naturalistic field operational test (FOT) data collected in the Gothenburg area at the end of 2014 and the beginning of 2015. Ten instrumented Volvo cars were used by employees and their families for everyday driving. The aim was to study a prototype system measuring driver visual attention, using cameras to detect the driver's gaze direction (on–/off-road). Though the cars were equipped with driver assistance systems, these systems were not enabled during

baseline data collection, which was the only part of the data set considered in this paper.

For the present analyses, the entire set of baseline data was filtered to extract all potential lane departure events. The following conditions were applied:

- Lateral distance from the middle of the car to the closest lane marker < 0.7 m (corresponding to the side of the car crossing the lane marker by > 0.2 m) for at least 0.3 s to ensure the presence of an actual exit from the driving lane.
- Lane width between 2.5 m and 4 m to avoid minor roads without lane markings and large open spaces.
- Speed > 50 km/h to exclude low-speed, possibly complex events.
- Road curvature > 500 m to avoid events on curved roads.
- No complete lane change occurred (i.e., the vehicle returns to the original lane after the event).

In total, 131 potential lane departure events matching the above criteria were extracted. Next, these events were examined by the authors who watched the front-view vid***eos. Nearly all excluded events were clear examples of intentional departures, such as when drivers made space for oncoming traffic in the adjacent lane or lanes were merging. If intentionality was unclear the cases were excluded.

The final data set included 34 unintentional lane departure events, extracted from 26 trips by six drivers. Three drivers were responsible for 90 % of the events.

2.1.2. The strategic highway research program 2 (SHRP2) data set

A naturalistic driving data set involving more than 3000 volunteer passenger-vehicle drivers (both males and females, in the age range 16–98 years) was collected over three years within the Strategic Highway Research Program 2 (SHRP2; Hallmark et al., 2014; Academies and of Sciences, Engineering, and Medicine, 2011). The collected real-world lane departures make up the basis of the second data set analyzed in this work. There were 1056 lane departures in this set, of which 1055 were considered crashes or near-crashes (see the report by Hankey et al., 2016 for the exact definition of crash and near-crash). The remaining event, annotated as "Crash-Relevant", was excluded. The 1055 crashes and near-crashes were filtered further to include only drift events with a minimal number of confounding factors; see Appendix A for full details. The filtering resulted in a set of 126 potential lane departure events.

Of these, 90 low-speed events (<50 km/h) were excluded from the data set. The remaining 36 potential lane departures were examined by studying each event's forward-view vid***eo and narratives (i.e., free-text event descriptions). In this step, a further 10 events were excluded. In addition to the selection criteria described earlier, speed and GPS data had to be available (necessary for the data preprocessing, see Section 2.2). Missing data resulted in another 20 events being excluded.

Only six events (five drivers with one event each, and one driver with two events) remained in the final data set. Three of these events lacked information about the vehicle's lateral lane position. For these cases, the lane position was retrieved using a vid***eo-based annotation tool (Shams El Din, 2020). The low number of remaining events may seem surprising, not least compared to the number of events extracted from the EyesOnRoad data set. However, it should be noted that the EyesOnRoad events were not near-crashes or crashes, like the events in the SHRP2 database. If the SHRP2 database had also included lower-criticality events, there would undoubtedly have been more. However, as noted, most of the original 1056 SHRP2 departures were low-speed events or influenced by complicating factors.

2.1.3. The run-off-road simulator study data set

This data set came from a study with 12 drivers (between 25 and 43 years old; nine males and three females) who were exposed to an artificially induced road departure event while driving on a highway in a full-motion, high-fidelity driving simulator. Full details about the artificially applied yaw angle and study setup are provided by Eriksson et al. (2018). While driving, the drivers had to perform a visual-manual secondary task involving reading numbers from a display on six occasions. Throughout the secondary task, one finger had to be touching the display for at least 2.2 s. A road departure event towards the right road edge was induced two times during the drive, coinciding with the performance of the secondary task. The departure event was accomplished by rotation of the displayed virtual environment until the vehicle had a 3° yaw angle relative to the road, without any vestibular or haptic feedback. Since the drivers were concentrating on the secondary task display, they did not notice the sudden visual change on the simulator screen. Hence, when they looked back toward the forward roadway, they were surprised by an imminent road departure.

The drivers' recovery maneuvers differed for the first (unexpected) road departure event and the second (repeated) event (Eriksson et al., 2018). To avoid possible learning effects, only the first (unexpected) events were included in the final data set used in this paper.

2.2. Data preprocessing

All events had to be preprocessed to permit the study of the timing and amplitude of the primary corrective steering adjustment. In this section, the methods are described for (1) defining gaze on–/off-road for each data set, (2) extracting individual steering adjustments, and (3) identifying the primary corrective steering adjustment in each event.

Unfortunately, the steering wheel angle was not available for all events. Hence, steering was quantified as the yaw rate relative to the road heading (referred to here as the relative yaw rate) throughout. Thus, the vehicle's rotation in relation to the world was used as a surrogate for steering wheel rotation and, consequently, as a proxy for the driver's reaction. Since, on a straight road, the relative yaw rate of the vehicle is approximately a delayed linear scaling of the steering wheel angle, the use of relative yaw rate as a surrogate has few practical implications for quantifying steering amplitude, but the observed steering timing will be delayed by about 0.05 – 0.2 s

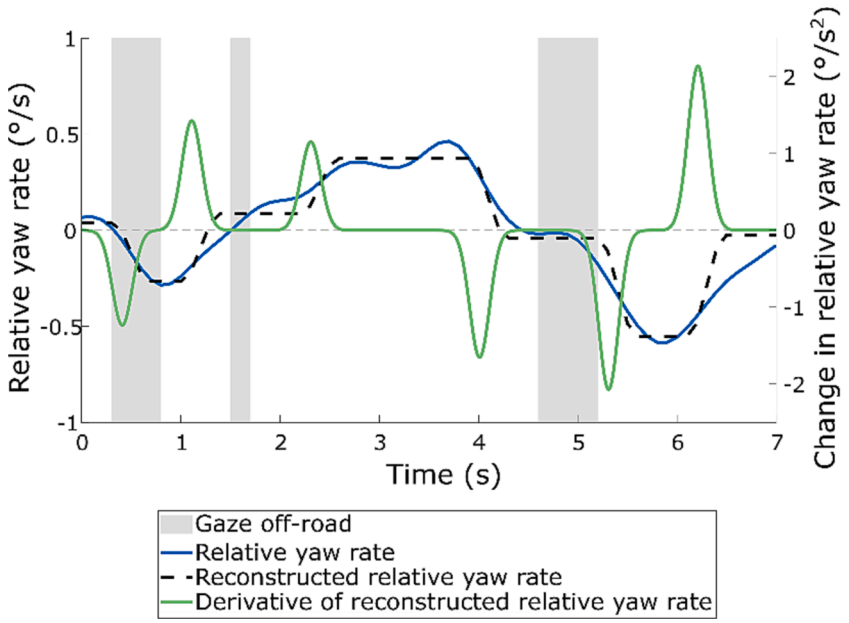

Fig. 2. A comparison between the original (blue) and reconstructed (black, dashed) relative yaw rate signal for one of the lane departure events in the EyesOnRoad data set. The change in relative yaw rate signal (green) based on bell-curve shaped adjustments is plotted on top of the comparison. Each peak in this signal corresponds to a distinct steering adjustment. (For interpretation of the references to colour in this figure legend, the reader is referred to the web version of this article.)

(Cao et al., 2013; Zhu et al., 2013). For the naturalistic data sets, the relative yaw rate was calculated by fusing data from the vehicle's GPS and yaw rate sensor; see Appendix B for details.

2.2.1. *Gaze direction*

The nature of the recorded gaze information differed between the data sets, including some differences in the definitions of on– and off-road gazes. The gaze data specifications for each data set are highlighted below.

The EyesOnRoad data set: This data set provided a Boolean signal stating whether the gaze was on– or off-road. Gaze was considered on-road when directed toward a rectangular area +/- 10° horizontally and +/- 10° vertically from a horizontal center line through the driver seat. The gaze direction was captured by an in-vehicle camera assisted by two infrared illumination modules (Karlsson et al., 2016).

The SHRP2 data set: The gaze direction was manually coded per vid***eo frame (15 Hz) by trained data annotators using vid***eo recordings of the drivers' faces. Each frame was associated with a discrete glance location (e.g., "forward", "center stack", or "rear-view mirror"). In this paper, gaze on-road corresponded to the "forward" glance location, defined as: "Any glance out the forward windshield directed towards the direction of the vehicle's travel. When the vehicle is turning, these glances may not be directed directly forward but towards the vehicle's heading" (Virginia Tech Transportation Institute, 2019).

The Run-off-road simulator study data set: A commercial (SmartEye; SmartEye, n.d.) four-camera eye tracker system was used to track the drivers' gaze directions. The driver's gaze was considered on-road when detected within an area of interest called "on-screen" and directed along the vehicle's heading.

2.2.2. *Steering adjustment extraction*

Steering control can be assumed to be an intermittent process that can be modeled as a sequence of ballistic motor primitives described, for example, by bell-shaped steering pulses (Benderius & Markkula, 2014; Cheng et al., 2020; Markkula et al., 2018). Consequently, in this paper, the steering rate is assumed to consist of a series of (possibly partially overlapping) bell-shaped adjustments, each with a duration of 0.4 s in accordance with previous literature (Benderius & Markkula, 2014; Markkula et al., 2018). Fig. 2 shows an example of a sequence of bell-shaped steering adjustments and the corresponding reconstructed relative yaw rate signal from the EyesOnRoad data set. A brief sensitivity analysis showed that small changes in the steering adjustment duration did not influence the methods (subjectively judged) accuracy noticeably.

Due to the intermittent nature of the steering signal, individual steering adjustments were extracted to reproduce the steering signal. Such extraction has previously been demonstrated by Markkula et al. (2018) using the steering wheel angle signal. The method from that study was here applied to the relative yaw rate signal (see the full paper by Markkula et al., 2018, for details on the steering adjustment extraction).

The steering adjustment extraction method developed by Markkula and colleagues (2018) is sensitive to small fluctuations in the steering signal. As in the original method, a Gaussian kernel averaging filter (also called Gaussian smoothing, see, e.g., Hastie et al.,

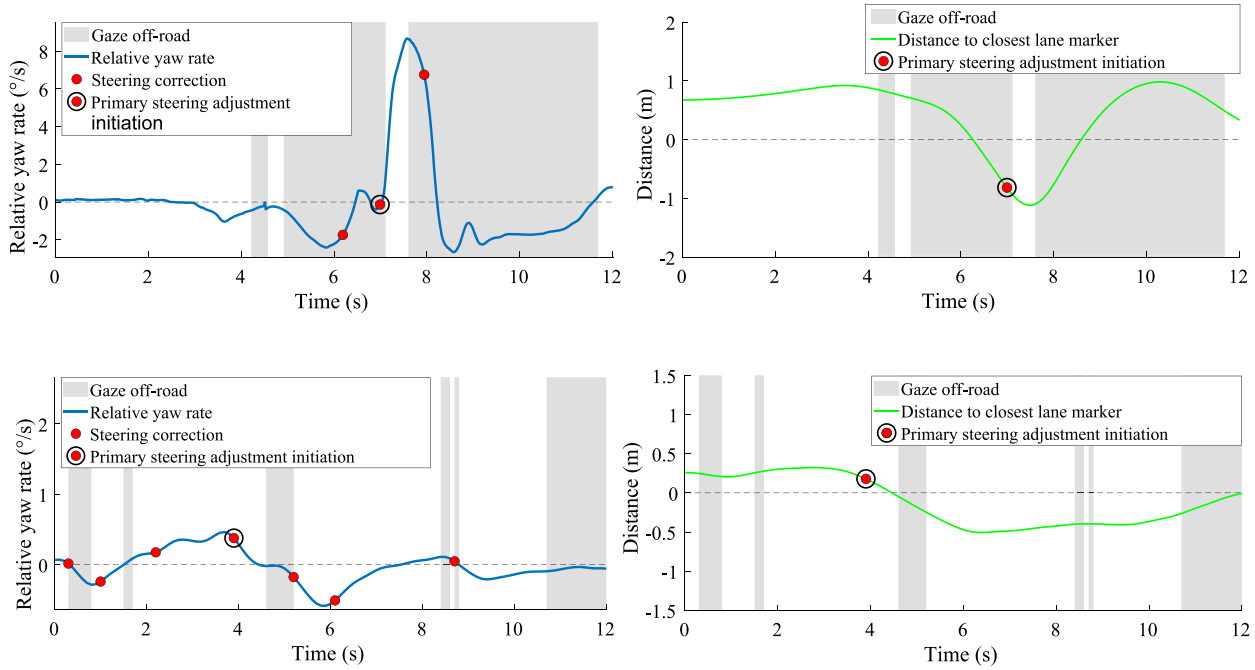

Fig. 3. Examples of the relative yaw rate signal and extracted steering adjustment initiations (left), as well as the corresponding vehicle position in the lane for the same events (right). The identified primary corrective steering adjustment of each event is encircled. Note the different vertical axes. *Upper panel:* A lane departure event from the Run-off-road simulator study data set. *Lower panel:* A lane departure event from the EyesOnRoad data set.

2009) was used to smoothen the relative yaw rate signals in all data sets. To balance the signal reconstruction error and the risk of overfitting the steering peaks, they concluded that using a filter with a standard deviation of 0.1 s was suitable for their lane-keeping data set (in the current study we use 0.11 s). However, the three data sets differed in the noise filtering required. Thus, after signal smoothing, a different minimum threshold for steering amplitude (i.e., a minimum value of the change in relative yaw rate) was defined for each data set. The purpose of the threshold was to closely replicate the original relative yaw rate signals. Small values were chosen for the naturalistic data sets (EyesOnRoad: 0.25°s^{-2}; SHRP2: 0.7°s^{-2}), while a relatively high value was necessary for the simulator data set (6°s^{-2}) to avoid identifying any part of the artificially applied yaw angle deviation (which was always less than 6 °s^{-2}) as the primary corrective steering adjustment. This choice did not have a major influence on the results since the drivers' primary corrective steering adjustments (quantified in terms of the change in relative yaw rate) in the simulator data set generally had high amplitudes (approximately in the order of 10–60°s^{-2}). Fig. 3 compares the relative yaw rate signal and the identified adjustments for an event from the simulator study data set and an event from the EyesOnRoad data set. It can be seen that the reconstruction is not perfect; some of the adjustments in Fig. 3 are longer than 0.4 s—or they consist of multiple overlapping adjustments in rapid succession, interpreted by the algorithm as a single adjustment. Therefore, the adjustments estimated timing may be delayed by 0.1–0.2 s. The magnitude of the steering adjustment is unaffected by possible timing delays.

2.2.3. Identification of the primary corrective steering adjustments

The primary corrective steering adjustment was defined as the first steering adjustment in the opposite direction of the lane departure. For the Run-off-road simulator study, adjustments to the yaw rate due to the artificially induced road departure were excluded; moreover, remaining adjustments were only considered as candidates for the primary corrective adjustment if they occurred after the artificial yaw rate application was complete. Examples of the primary corrective steering adjustments identified in two events, one from naturalistic data and one from the simulator study, can be found in Fig. 3. The initiation time of the primary corrective steering adjustment, defined as the start of the corresponding bell-shaped curve, was analyzed in relation to the end of the last off-road glance that the driver initiated before the steering adjustment.

The bulk of the analyses in this paper concern the amplitude of the primary corrective steering adjustment, which is defined as the change in relative yaw rate at the peak of the bell-shaped curve (i.e., halfway through the primary corrective steering adjustment). The analysis of the amplitude will be described in the next section.

2.3. Lane departure risk metrics

The steering amplitude was described in relation to a set of lane departure risk metrics, measured at the initiation of the primary corrective steering adjustment. The drivers are assumed to use these risk metrics to evaluate the momentaneous lane departure risk in a

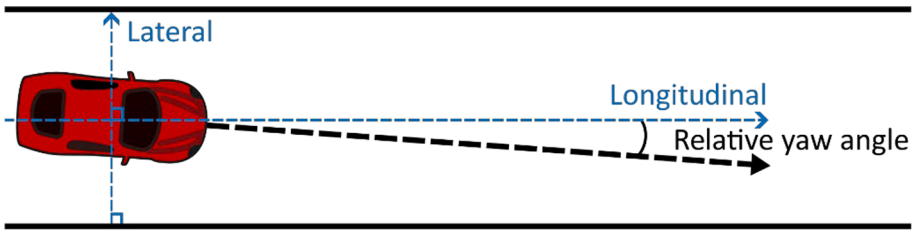

Fig. 4. An illustration of relative yaw angle.

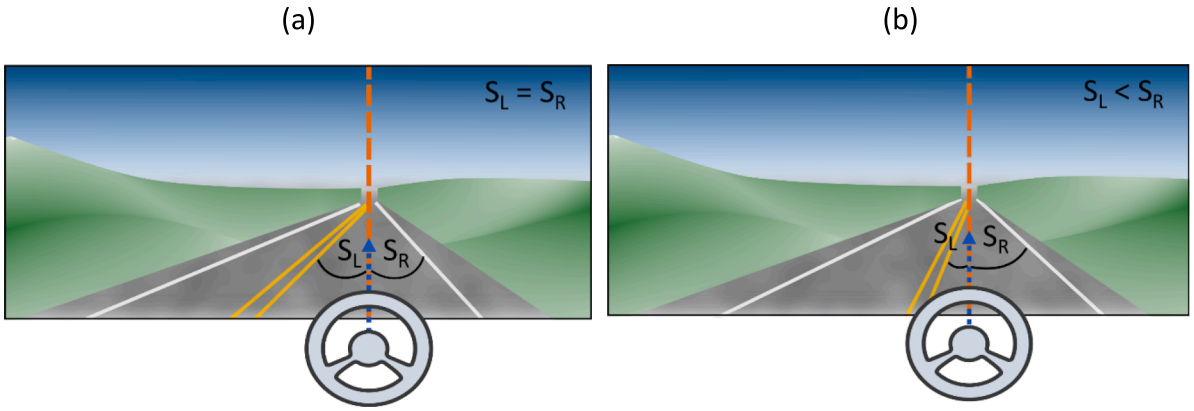

Fig. 5. Simplified illustrations of splay angles in a straight-road driving situation. *Panel a*: The vehicle is driving straight in the middle of the lane. *Panel b*: The vehicle is driving straight close to the left lane boundary.

given situation, and, consequently, the need for an immediate steering response. Since drivers mainly use visual stimuli to guide their actions (Macadam, 2003), only risk metrics which were possible to perceive visually (directly or indirectly) were considered, and no vestibular or haptic cues were investigated. All three data sets included only straight roads or very mild curves. Thus, for simplicity, zero road curvature was assumed in all risk metric calculations, along with a fixed vehicle width of 1.8 m. The vehicle's front axis was assumed to be positioned 1 m from the vehicle center (Mammar et al., 2006).

In this study the following risk metrics were used: relative yaw angle, risk metrics based on splay angle (three alternatives), risk metrics based on critical yaw rate (three alternatives), and modified iTLC. They are described here in turn.

2.3.1. *Relative yaw angle*

The relative yaw angle θ, illustrated in Fig. 4, is defined as the difference in degrees between the vehicle's forward direction and the lane's forward direction (at the vehicle's location). It may be considered a very simple lane departure risk metric, since it is independent of the estimated time or distance to departure. That is, the vehicle may be positioned at any lateral distance from the lane marker with the same relative yaw angle.

2.3.2. *Risk metrics based on splay angle*

The splay angle is the angle between the optical projection of a straight path and the vertical and has been used to explain the control of alignment in aviation (Calvert, 1954; Warren, 1982). In the car driving context, the splay angle is defined as the angle between a vertical line and the optical projection of lane markers on the driver's retina (Beall & Loomis, 1996; L. Li & Chen, 2010). This angle provides information about the vehicle's lateral position, independent of potential look-ahead distance (comparable to looming in a longitudinal situation; Lee, 1976; Svärd et al., 2017, 2021). Using splay angles as a risk metric is attractive since they are directly available in the driver's visual input. Angular information is efficiently acquired and processed by the human brain because of the spatial organization of neurons in the primary visual cortex (Martínez-García & Gordon, 2018; Yacoub et al., 2008). Fig. 5 provides illustrations of splay angles in two different situations.

Splay angles towards both the left and the right were calculated under the simplifying assumption that the driver was laterally positioned in the middle of the vehicle. This assumption is motivated by the hypothesis that the driver has learned to adjust for the contribution to the splay angles from their off-central placement in the vehicle. This definition also makes the metric easier to interpret because the left and right splay angles are equal when the vehicle is in the middle of the lane (independent of the vehicle's rotation). Furthermore, the driver's eyes were assumed to be at the height of $h_{eyes} = 1.1$ m from the ground. The splay angle S can then be written as in Equation (1):

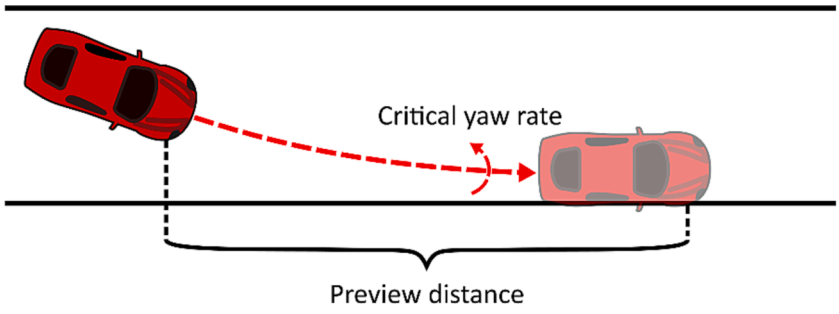

Fig. 6. An illustration of critical yaw rate.

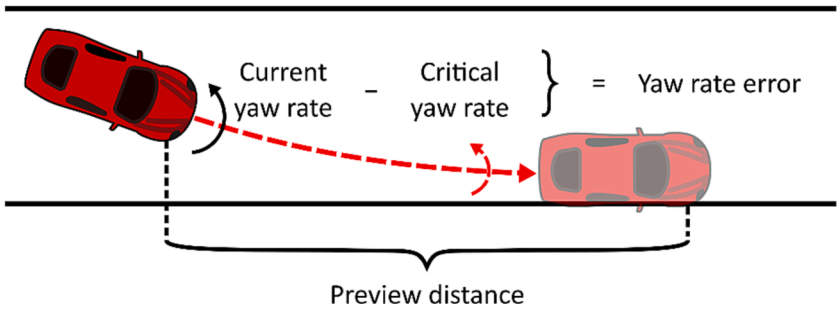

Fig. 7. An illustration of yaw rate error. The red dashed line depicts the estimated vehicle trajectory corresponding to the critical yaw rate, with the front right tire of the car exiting the line at the preview distance. (For interpretation of the references to colour in this figure legend, the reader is referred to the web version of this article.)

$$S = \tan^{-1}\frac{d_{lm}}{h_{eyes}\cos\theta} \tag{1}$$

where d_{lm} is the lateral distance to the lane marker, and θ is the relative yaw angle (L. Li & Chen, 2010).

Three lane departure risk metrics were defined based on splay angle information:

Splay angle with respect to the closest departure direction, S_R or S_L: This risk metric is defined as the splay angle in the departure direction—that is, the splay angle with respect to the right-lane marker, S_R, for departures towards the right and the splay angle with respect to the left-hand lane marker, S_L, for departures towards the left of the lane.

Splay error, S_{err}: This risk metric compares the left and right splay angles, as shown in Equation (2). This metric has previously been used in steering controls. A value close to zero reflects a steady lane position in the middle of the lane (Martínez-García & Gordon, 2018).

$$S_{err} = S_R - S_L \tag{2}$$

Change in splay error, $\dot{S}_{err}$: This risk metric is defined as the derivative of the splay error with respect to time.

2.3.3. Risk metrics based on critical yaw rate

The critical yaw rate $\dot{\theta}_c$ is defined as the yaw rate that, if sustained, would result in lane departure at a specific preview distance d_p and preview time t_p (Gordon et al., 2009; Martínez-García et al., 2016; Martínez-Garcia & Gordon, 2017). The preview time can be understood as the driver's look-ahead time (how far ahead the driver plans their driving). Commonly used preview times of 1–3 s (Gordon & Srinivasan, 2014; Martínez-García & Gordon, 2018; Ungoren & Peng, 2005) motivated the four preview time alternatives selected in this paper: 0.5 s, 1 s, 1.5 s, and 2.5 s.

Three lane departure risk metrics based on critical yaw rate were explored:

Critical yaw rate, $\dot{\theta}_c$: When the critical yaw rate was directly used as a risk metric, it was defined with respect to the closest lane boundary (on the right for right-hand side departures and on the left for left-hand side departure events); see Fig. 6. The critical yaw rate was calculated according to Equation (3). This metric may, theoretically, take on both positive and negative values depending on whether vehicle is estimated to depart from the lane earlier or later than the defined preview time:

$$\dot{\theta}_c = \frac{2v\sin(\phi)}{d_p} \tag{3}$$

In Equation (3), v is the vehicle speed, ϕ is the angular difference between the current yaw direction and the preview point at the

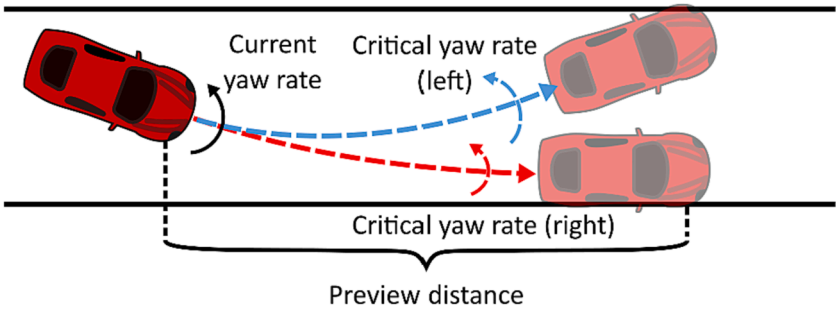

Fig. 8. An illustration of critical normalized yaw rate. The dashed lines depict the estimated vehicle trajectories corresponding to the left (blue) and right (red) critical yaw rate, with the front left or right tire of the car exiting the lane at the preview distance. In the depicted scenario, the vehicle would have departed from the lane to the right at a distance shorter than the preview distance (and not departed the lane at all to the left), had the current yaw rate been sustained. Thus, in this case, both the right and left critical yaw rate would rotate the vehicle toward the left to make it depart the (left or right) lane at the predefined preview distance. (For interpretation of the references to colour in this figure legend, the reader is referred to the web version of this article.)

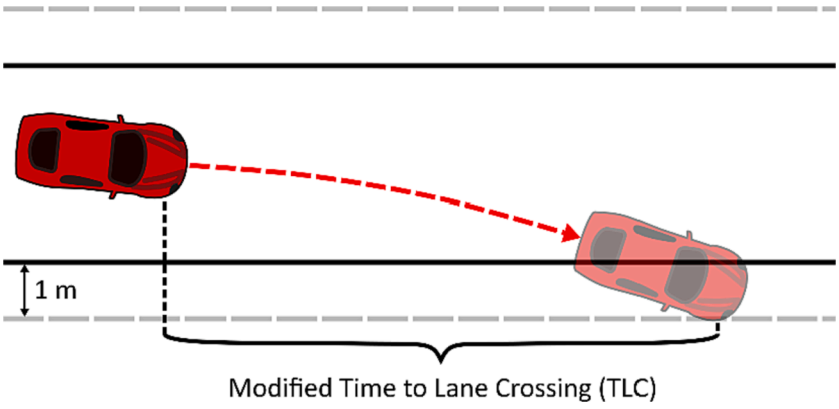

Fig. 9. An illustration of modified TLC, with the artificial lane markers as dashed grey lines.

lane boundary, and d_p is the distance (in meters) to the preview point (Gordon et al., 2009; Martínez-García et al., 2016; Martínez-García & Gordon, 2018).

Yaw rate error (YRE): The YRE metric, shown in Equation (4), is the difference between the current and critical yaw rates. It addresses a shortcoming of the critical yaw rate, which does not consider the current yaw rate. YRE is measured with respect to the closest lane boundary; see Fig. 7. The YRE has previously been suggested to measure lane-keeping performance (Gordon et al., 2009).

$$\boldsymbol{YRE} = \dot{\boldsymbol{\theta}} - \dot{\boldsymbol{\theta}}_{\boldsymbol{c}} \tag{4}$$

where $\dot{\boldsymbol{\theta}}$ is the current relative yaw rate.

Critical normalized yaw rate (CNYR): The CNYR is a further refinement of the critical yaw rate and YRE risk metric which takes both sides of the lane into account; see Fig. 8 and Equation (5). Moreover, it is normalized. The driver is required to keep $|CNYR| < 1$ to stay within the lane during the defined preview time. This measure has been previously used in computational models of drivers' lane-keeping behaviors (Martínez-García et al., 2016; Martínez-García & Gordon, 2018). CNYR is calculated as follows:

$$\text{CNYR} = \frac{\dot{\boldsymbol{\theta}} - 0.5(\dot{\boldsymbol{\theta}}_{\boldsymbol{c,L}} + \dot{\boldsymbol{\theta}}_{\boldsymbol{c,R}})}{0.5(\dot{\boldsymbol{\theta}}_{\boldsymbol{c,L}} - \dot{\boldsymbol{\theta}}_{\boldsymbol{c,R}})} \tag{5}$$

In Equation (5), $\dot{\theta}_{c,L}$ is the critical yaw rate with respect to the left-hand side and $\dot{\theta}_{c,R}$ is the critical yaw rate with respect to the right-hand side of the lane.

2.3.4. Modified iTLC

Time to collision (TTC) and its inverse are common measures of situational criticality for longitudinal driving situations (Kiefer et al., 2005; Kondoh et al., 2014; D. N. Lee, 1976). Time to lane crossing (TLC) can be considered a counterpart for lateral situations (Godthelp, 1988; Mammar et al., 2006; van Winsum et al., 2000). It has been shown that the reciprocal of TLC, inverse time to lane crossing (iTLC), is associated with the perceived risk of lane exceedance (Boer, 2016; Cheng et al., 2020). Thus, a high iTLC value may

trigger a corrective steering action.

A weakness of using iTLC as a lane departure risk metric in the context of the present analyses is that it would be undefined as soon as the driver departs from the lane, resulting in missing data on the occasions where the driver does not initiate the primary corrective steering adjustment until after the vehicle has already crossed the lane marker. Therefore, a modified version of iTLC was used. The modified iTLC was defined as the inverse of the estimated time to cross an artificial lane marker positioned one meter beyond the actual lane marker; see Fig. 9.

The modified iTLC, $iTLC_{mod}$, was estimated using the method for calculating TLC based on lateral position, speed, and an assumed constant acceleration described by Mammar et al., (2006; see also P. Li et al., 2018), as shown in Equation (6),

$$iTLC_{mod} = \frac{a_{lat}}{-v_{lat} + \sqrt{v_{lat}^2 + 2a_{lat}(d_{lat}+1)}} \tag{6}$$

where d_{lat} is the lateral distance from the closest lane marker, v_{lat} is the lateral speed (i.e., speed towards the lane marker), and a_{lat} is the constant lateral acceleration (i.e., acceleration towards the lane marker).

2.4. Model selection

Bayesian linear regression was used to investigate whether it was possible to construct a model which could accurately estimate the amplitude of the primary corrective steering adjustment (Gelman et al., 2013; Sosa & Aristizabal, 2022). A set of candidate steering amplitude models were devised using the lane departure risk metrics presented in Section 2.3. Some risk metrics were closely correlated due to sharing a common basis (e.g., all splay angle-based risk metrics). However, only metrics that were not based on the same concept were used as predictors in the same candidate model.

Equations (7a)–c show the structure of the Bayesian linear model that was applied in this work. Non-informative (very vague) conjugate priors were assumed (Koch, 2007; Lambert, 2018). Similar to what was suggested by Lynch (2007), the predictor coefficients, $\boldsymbol{\beta}$, were sampled from a very flat normal distribution (i.e., centered around zero with a variance of 10^6). Moreover, the model variance, $\boldsymbol{\sigma}^2$, was sampled from a conjugate inverse gamma prior distribution with small hyperparameters (shape and rate set to 0.001; Lunn et al., 2012). The model can be expressed as:

$$\ddot{\boldsymbol{\theta}}|\boldsymbol{x},\boldsymbol{\beta},\boldsymbol{\sigma}^2 \; \mathcal{N}\left(\boldsymbol{\beta}_0 + \boldsymbol{\beta}_1\boldsymbol{x}_{1,i} + \boldsymbol{\beta}_2\boldsymbol{x}_{2,i} + \cdots + \boldsymbol{\beta}_k\boldsymbol{x}_{k,i}, \boldsymbol{\sigma}^2\right), \boldsymbol{i} = 1, 2, \cdots, \boldsymbol{n} \tag{7a}$$

$$\boldsymbol{\beta}_j \; \mathcal{N}\left(0, 10^6\right), \boldsymbol{j} = 1, 2, \cdots, \boldsymbol{k} \tag{7b}$$

$$\boldsymbol{\sigma}^2 \; \mathcal{IG}(0.001,\ 0.001) \tag{7c}$$

where $\ddot{\theta}$ is the change in relative yaw rate, $\boldsymbol{x}$ is the predictor vector, k is the number of predictors in the model, and n is the number of observations.

The candidate model predictors were chosen based on Spearman's correlation coefficient, ρ, between the corresponding risk metric and the change in relative yaw rate. The model selection was then based on forward elimination (James et al., 2017). The method involves keeping predictors for which the highest posterior density (HPD) interval is non-overlapping with zero and incrementally add predictors until the adjusted R^2 value (henceforth denoted by R^{-2}), estimated with Wherry's formula (Wherry, 1931), no longer improves. That is, until the proportion of data explained by the model no longer increases, when adjusted for model complexity.

In an attempt to further improve the model, polynomial predictor terms were added to the model candidates in the last selection step. The polynomial terms were used to further investigate the influence of higher order terms of the dominating model predictors (see Appendix C for details). Prior to adding a polynomial predictor term, the polynomial was linearly transformed into an orthogonal polynomial (Narula, 1979, provides an overview of orthogonal polynomials in regression). The orthogonality transformation was necessary to make the polynomial predictors linearly independent. In the model selection process, the composite predictors were kept or discarded under the same conditions as the single predictors (i.e., adding or removing the predictors one by one).

Finally, a threshold model (i.e., a model describing two different dynamic processes—one below, and one above—a certain threshold) depending on the was suggested based on the results from fitting the linear (and polynomial) models to our three data sets. The threshold model used in this work was locally linear, with a threshold on the relative yaw angle determining the shift between two different processes: one process for less critical situations and one process more critical situations.

All models were evaluated using the JAGS package in R (JAGS, n.d.), using Markov Chain Monte Carlo (MCMC) sampling with three chains.

3. Results

The first subsection below presents the results from the analyses of the timing of the primary corrective steering adjustments from unintentional lane departures in the three data sets. The next subsection describes the analysis of the suggested lane departure risk metrics and the results of using these metrics to model the primary corrective steering amplitudes. An overview of the adjustment timings and amplitudes, overall and for each data set separately, is presented in Table 2.

Table 2
An overview of the timing and amplitude of the primary corrective steering adjustments, overall and per data set.

Data set	No. of departures (left / right)	Steering response time from glance on-road, mean (std), [s]	Steering amplitude, mean (std), [s^{-2}]
EyesOnRoad	16 / 18	0.58 (0.98)	−1.09 (0.66)
SHRP2	3 / 3	0.38 (0.60)	−4.33 (2.88)
Run-off-road simulator study	0 / 12	−0.06 (0.28)	−26.67 (13.91)
All	19 / 33	0.40 (0.86)	−7.37 (12.56)

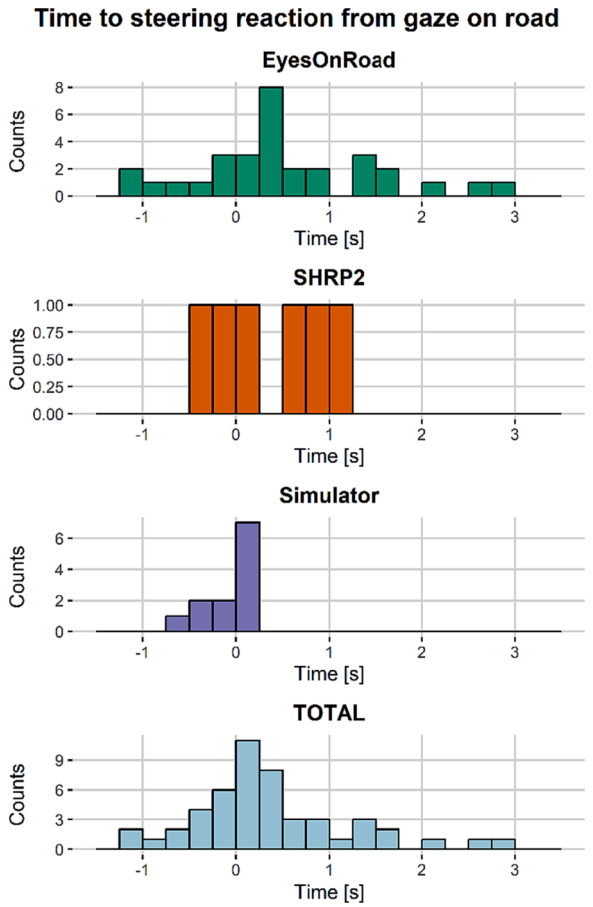

Fig. 10. Distributions of steering initiation times (measured from the end of the last off-road glance before the primary corrective steering adjustment). The upper three panels present the distributions for each studied data set separately, while the panel at the bottom provides the total distribution over all data sets. Note that negative time values correspond to steering adjustments initiated before the driver's gaze returned to the road.

3.1. Initiation of the primary corrective steering adjustment

The distributions of the time between the end of the last off-road glance and the initiation of the primary corrective steering adjustment are presented in Fig. 10. It can be observed that a large proportion of drivers initiated their steering response before, or at the same time as, they redirected their gaze towards the road in front.

Some differences between data sets were observed. Drivers in the simulator study reacted earlier than drivers in the naturalistic data (EyesOnRoad and SHRP2). Practically all drivers in the simulator study had started to steer before looking up (the yaw rate change was initiated within 0.25 s of the time that the gaze returned to the road), while the drivers in the EyesOnRoad data set had a high number of steering reactions occurring just after looking up (0.25–0.5 s after the gaze was back on the road). Similarly, 50 % of the SHRP2 drivers (i.e., three drivers) reacted before looking up, and 50 % initiated steering at a later point in time.

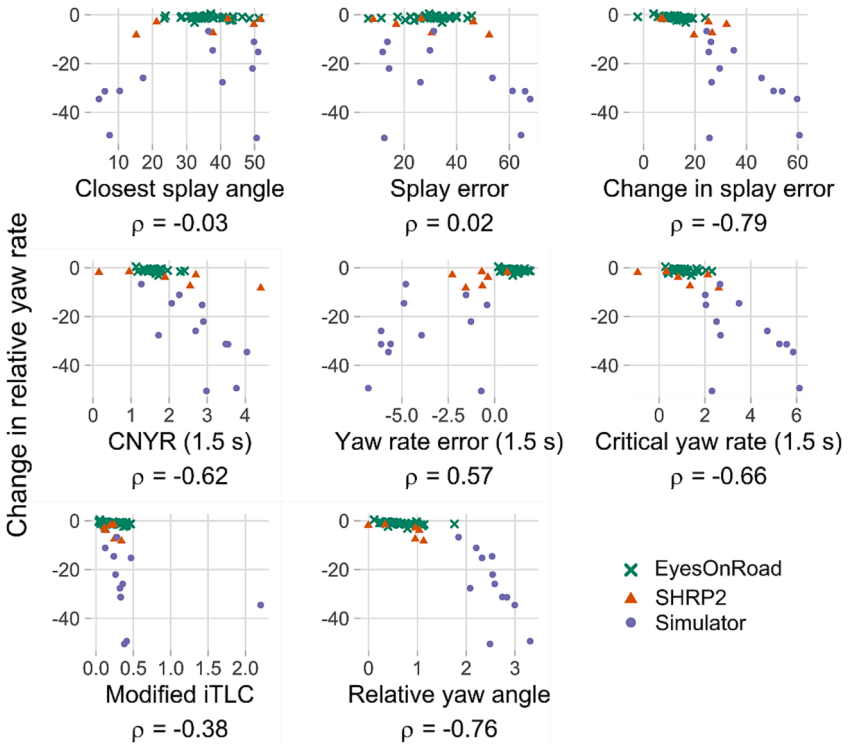

Fig. 11. Lane departure risk metrics for all events, plotted against the corresponding change in relative yaw rate. Note that the lane departure risk metrics are plotted independently of departure direction. That is, only the absolute values of the risk metrics are shown. Note that, for clarity reasons (i.e., reducing clutter), the CNYR, yaw rate error, and critical yaw rate risk metrics with corresponding preview times 0.5 s, 1.0 s, and 2.5 s are omitted from the illustration.

3.2. Lane departure risk metrics and steering amplitude

The below subsections present the results from the analysis of lane departure risk metrics and describe how the metrics may be associated with the primary corrective steering adjustment amplitude. The best-performing Bayesian regression models are also described. Full details of the model selection process are presented in Appendix C.

3.2.1. Drivers' responses to lane departure risk metrics

Scatter plots of the risk metrics and corresponding steering amplitudes are shown in Fig. 11. Apparent differences in responses between the data sets could be observed, with the most evident correlations (in terms of ρ-value) between risk metrics and steering amplitudes emerging from the simulator data set. However, considerable response variations can be seen between individual data points, as well as between data sets.

3.2.2. Linear model performance

The best model for predicting steering amplitudes across all three data sets using only linear modeling terms ($R^{-2} = 0.75$) was based on the relative yaw angle as the only predictor, as shown in Equation (8):

$$\ddot{\boldsymbol{\theta}} = \boldsymbol{\beta}_0 + \boldsymbol{\beta}_1\boldsymbol{\theta} \tag{8}$$

The output $\ddot{\theta}$ is the change in relative yaw rate at the peak of the primary corrective steering adjustment. The model was fitted using three MCMC chains with 100,000 iterations each (burn-in: 5,000), reaching good convergence.

The bottom part of Panel a in Fig. 12 illustrates the 95 % HPD interval of the predictor coefficient (β_1), which turned out to be well separated from zero (i.e., the predictor clearly contributes to the model fit). The mean value was $\beta_1 = -12.38$. The model output is illustrated by a straight line in the upper part of the panel, together with the actual data points from all three data sources. It can be observed that this linear model predicts the amplitude of the primary corrective steering adjustment reasonably well for all data sets but does not capture potential non-linearities in the data.

The performance of the model in Equation (8) considerably decreased when fitted to the data from the simulator study only ($R^{-2} = 0.26$), which are much better explained by the linear relative yaw angle-based model ($R^{-2} = 0.48$). However, the linear relative yaw angle-based model performed poorly on the naturalistic data sets ($R^{-2} = 0.14$). A better fit to the naturalistic data ($R^{-2} = 0.33$) was obtained using a linear model based on the change in splay error. Fig. 12, Panel b, illustrates how this change-in-splay-angle-based

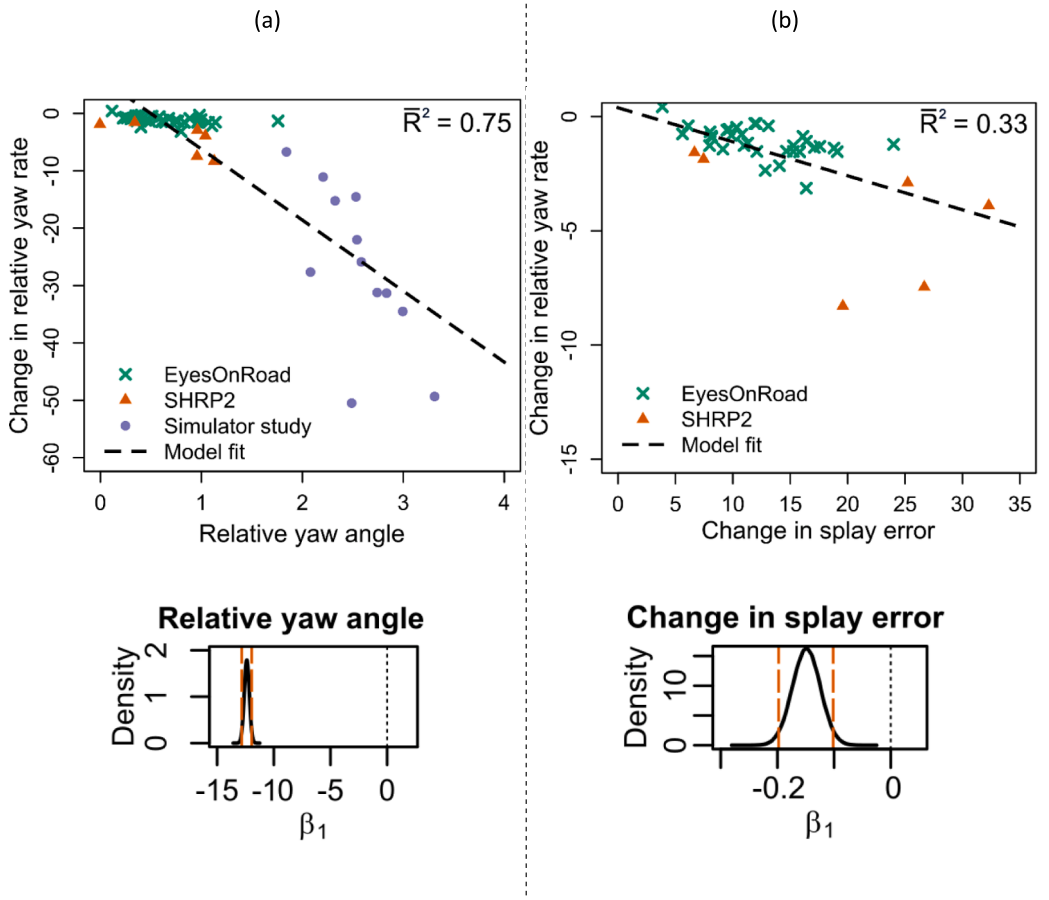

Fig. 12. Illustrations of how the best-performing linear models (black dashed lines) fit to the data sets. Posterior density plots of the model predictor coefficients are shown at the bottom of each panel. The orange dashed lines represent the boundaries of the 95 % HPD interval, and the dotted black line marks the position where the horizontal axis crosses zero. *Panel a:* A model based on the relative yaw angle, fitted to the full (combined) data set ($R^{-2} = 0.75$). *Panel b:* A model based on the change in splay error, fitted to the naturalistic data sets only ($R^{-2} = 0.33$). (For interpretation of the references to colour in this figure legend, the reader is referred to the web version of this article.)

model fits the naturalistic data. It also shows the posterior distribution of the predictor coefficient.

Overall, the change in splay error had the most impact on the naturalistic model fits, while the relative yaw angle predictor best explained the variations observed in the simulator data.

3.2.3. A polynomial model outperforms the best linear model

Even though linear models could predict the amplitude of the primary corrective steering adjustment reasonably well, it was possible to improve the model fit substantially by adding polynomial terms to the model equation. The best model fit over all data sets ($R^{-2} = 0.84$) was obtained from the polynomial model in Equation (9):

$$\ddot{\boldsymbol{\theta}} = \boldsymbol{\beta}_0 + \boldsymbol{\beta}_1\boldsymbol{\theta} + \boldsymbol{\beta}_2\boldsymbol{\theta}^2 \tag{9}$$

where the output $\ddot{\theta}$ is the change in relative yaw rate at the peak of the primary corrective steering adjustment, and the predictor θ is the relative yaw angle at the initiation of the adjustment. The model was fitted using three MCMC chains with 100,000 iterations each (burn-in: 5,000), reaching convergence.

The bottom part of Panel a in Fig. 13 shows that the 95 % HPD intervals of the predictor coefficients for both polynomial terms (β_1 and β_2) are well separated from zero. A linear transformation back to the original polynomial would yield the mean parameter values 5.83 and − 5.9 instead of − 77.73 and − 27.67. (The former values should be used when the model is applied directly to the relative yaw angle signal without first performing the orthogonality transformation required for the model selection process.) As illustrated in Panel a of Fig. 13, this polynomial model predicts the primary steering adjustment amplitude well.

However, the model performance seems to be heavily impacted by the data points from the simulator study. Fitting the same model *separately* to the naturalistic and simulator data sets reveals that the second-degree predictor no longer has an effect (the HPD interval crosses zero). The model fit to the separate data sets is considerably lower than that of the complete data set. Applying a linear model of

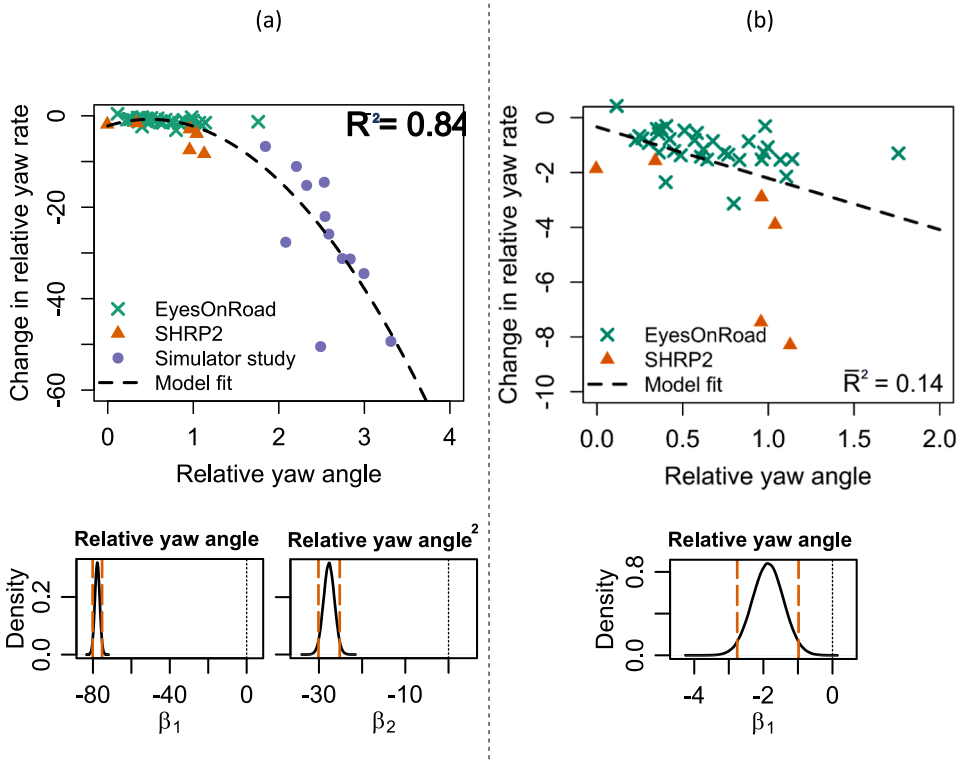

Fig. 13. *Panel a:* The relative yaw angle risk metric plotted against the change in relative yaw rate (colored markers), and the best polynomial model fitted to all data sets (dashed line; $R^{-2} = 0.84$). Posterior density plots of the model predictor coefficients are shown at the bottom of the panel. The dashed lines represent the boundaries of the 95 % HPD interval, and the dotted black line marks the position where the horizontal axis crosses zero. *Panel b:* The relative yaw angle risk metric plotted against the change in relative yaw rate (colored markers), together with a linear relative yaw angle-based model fitted to naturalistic data only (dashed line; $R^{-2} = 0.14$). A posterior density plot of the model predictor coefficient is shown at the bottom of the panel. The dashed lines represent the boundaries of the 95 % HPD interval, and the dotted black line marks the position where the horizontal axis crosses zero.

the relative yaw angle results in $R^{-2} = 0.14$ on the naturalistic data sets and $R^{-2} = 0.48$ on the simulator study data set. The model performance on the naturalistic data sets is shown in Fig. 13, Panel b.

3.2.4. A threshold model based on the best linear models has overall best performance

The previously described models based on the relative yaw angle perform best for high relative yaw angle values. For less critical cases (lower relative yaw angle values), a better fit is given by a model based on the change in splay error, as shown in Section 3.2.3. Further, a non-linear model component could potentially contribute to capture the difference in behavior between low and high relative yaw angle values (see Fig. 11). Therefore, we set up a threshold model, allowing different dynamics in the two relative yaw rate ranges:

$$\ddot{\boldsymbol{\theta}} = \begin{cases} \boldsymbol{\beta}_0 + \boldsymbol{\beta}_1 \dot{\boldsymbol{S}}_{\boldsymbol{Err}}, \theta < 1.2^{\circ} \\ \boldsymbol{\beta}_2 + \boldsymbol{\beta}_3 \theta, \theta \geq 1.2^{\circ} \end{cases} \tag{10}$$

The threshold used here was 1.5, but all values between 1.2 and 1.7 would give the same results since no data points exist in this interval. The model was fit to the combination of all data sets. The model performance (overall $\bar{R}2 = 0.85$) not only exceeded the performance of the polynomial model suggested in Section 3.2.4, but it also had a more even performance over all data sets with $\bar{R}2 = 0.34$ on the naturalistic data sets, and $\bar{R}2 = 0.44$ on the simulator data set, see Fig. 14. The optimal parameter set was: $\beta_0 = 0.4$, $\beta_1 = -0.15$, $\beta_2 = 40.31$, and $\beta_3 = -26.22$.

4. Discussion

This work investigated the timing and amplitude of drivers' primary corrective steering adjustments in unintentional lane departures due to lateral drift. The subsections below discuss the main conclusions drawn from the results and the most important limitations of the data and analyses.

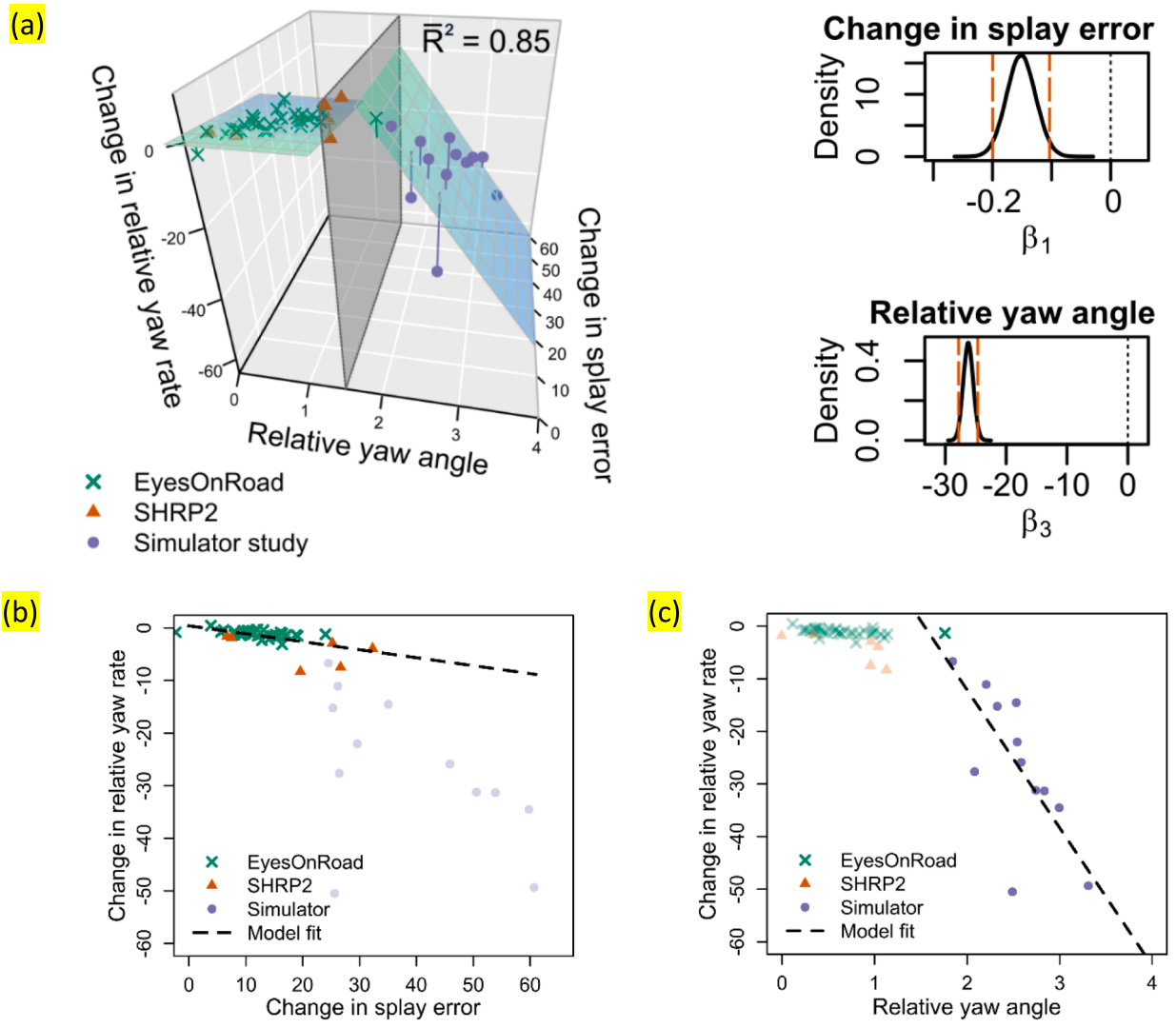

Fig. 14. *Panel a:* The change in splay error and relative yaw angle risk metrics plotted against the change in relative yaw rate (colored markers), and the best threshold model fitted to all data sets (colored surfaces; $R^{-2} = 0.85$). The threshold is illustrated by the grey transparent plane. Posterior density plots of the model predictor coefficients are shown in the right side of the panel. The orange dashed lines represent the boundaries of the 95 % HPD interval, and the dotted black line marks the position where the horizontal axis crosses zero. *Panel b:* The change in splay error risk metric plotted against the change in relative yaw rate. Data points corresponding to a relative yaw angle value less than 1.5 are displayed with colored markers, while data points corresponding to a relative yaw angle greater than or equal to 1.5 are represented by faded colored markers. The dashed line shows the threshold model fit for low yaw angle values. *Panel c:* The relative yaw angle risk metric plotted against the change in relative yaw rate. Data points corresponding to a relative yaw angle value greater than or equal to 1.5 are displayed with colored markers, while data points corresponding to a relative yaw angle less than 1.5 are represented by faded colored markers. The dashed line shows the threshold model fit for the higher range of yaw angle values. (For interpretation of the references to colour in this figure legend, the reader is referred to the web version of this article.)

4.1. Drivers often initiate the primary corrective steering adjustment initiation while still looking off-road

Most drivers initiated the primary corrective steering adjustment before, or at the same time as, they redirected their gaze toward the road in front. This interpretation is clearly not changed by the slight delay between the steering wheel adjustments and the yaw rate signal which was used in this analysis (mentioned in Section 2.2). On the contrary, an equivalent analysis of the steering wheel adjustments would have shown even earlier reactions.

Thus, the drivers could guide their steering response without using foveal vision, suggesting the use of peripheral vision. This finding corresponds to the steering-leads-gaze strategy in curve-taking described by (Lehtonen et al., 2018). The results are also consistent with studies showing that, in non-critical situations, lane-keeping is supported by peripheral vision, presumably providing the driver with information about lane edges and optic flow (Land & Horwood, 1995; Robertshaw & Wilkie, 2008). In a test track

experiment, Summala et al. (1996) tasked drivers with steering while keeping their gaze off-road; while their lane-keeping performance was degraded. They concluded that an experienced driver could still successfully keep the car in the lane using only peripheral vision. However, to the authors' knowledge, this type of peripherally guided steering has not been demonstrated for critical situations.

Although all data sets suggested that drivers may start steering while still looking away from the road, there were some differences in response times between data sets. The drivers in the naturalistic data sets exhibited somewhat later steering initiation than those in the simulator study. The EyesOnRoad data set had a small peak in response times between 0.25 s and 0.5 s (including the 0.05–0.2 s delay before the steering response was detectable as a change in relative yaw rate, as well as possible delays because of imperfect signal reconstruction, as mentioned in Section 2.2). Since typical response times in car driving range from 0.4 s to more than 1 s (Makishita & Matsunaga, 2008; Szydłowski et al., 2021), it would generally not be possible for the drivers to visually perceive the scene and decide to react based on that information in such a short time frame (Wolfe et al., 2019). However, it is reasonable to believe that the drivers' gaze was drawn back toward the road because of the detection of an imminent lane departure.

Another apparent difference between the data sets is the absence of long response times in the simulator study data. A potential reason for this is the study setup, which ensured that the drivers were visually distracted at the time of the lane departure event. Naturally, a similar control of the timing of the visual distraction was absent in the naturalistic driving data sets. In fact, a few very long response times (up to three seconds) were observed in naturalistic driving. In these events, the predominant cause of the vehicle movement towards the lane marker may not have been visual distraction, but could, for example, have been incapacitated or sleepy drivers (Cicchino & Zuby, 2017). Moreover, the severity of the events may have influenced the glance response times. In a highly time critical situation, the drivers cannot afford to postpone the corrective adjustment until more situational information has been accumulated. In contrast, in less-critical situations (e.g., those in the EyesOnRoad data set), the drivers have time to evaluate the situation before deciding to steer (at least in some events). Also in situations of equal *time* criticality, a high risk of serious consequences (e.g., serious injuries) may urge the driver to respond quicker than in a corresponding low risk situation (e.g., a situation where only minor property damage would be likely). In the high-risk situation, the driver would not want to delay the response, while the driver in the low-risk case could afford to properly assess the situation in spite of an increased departure risk.

4.2. Both a polynomial and a threshold model can explain the steering amplitudes from all data sets

Sections 3.2.3 to 3.2.5 demonstrated that the amplitudes of the primary corrective steering adjustments of all events in all considered data sets can be explained by one single, polynomial model, with good performance in terms of R^{-2} value. However, a threshold model explaining the data as the result of two different dynamical processes also achieved a high model fit. A shared property of both the polynomial and the threshold model was the use of the relative yaw angle at steering initiation as input, which was the least complex lane departure risk metric studied in this work. The models based on this simple metric outperformed models based on more complex risk metrics (such as the change in splay error, critical yaw rate, or modified iTLC).

A model using a second-degree polynomial of the relative yaw angle as a predictor reached a very high R^{-2} value (0.84). Interestingly, a mathematical analysis (derivation in Appendix D) shows that for any given lane departure scenario, the minimal required steering to avoid lane departure actually scales quadratically with the relative yaw angle. In other words, the second-degree polynomial relation between relative yaw angle and change in yaw rate suggests that drivers, in their first (primary) corrective steering adjustment, scale the amplitude of the steering adjustment as necessary to bring the vehicle back into the lane. This finding is consistent with the observations by Markkula et al. (2014), who concluded that steering to avoid collision with a lead vehicle was best described by an open-loop steering adjustment of a magnitude scaled with the requirements of the collision situation. Similar urgency-scaled driver responses have also been reported and used for modeling drivers' braking behaviors in critical lead-vehicle events (Svärd et al., 2017, 2021).

However, the polynomial relative yaw angle-based model did not reproduce the observed steering amplitudes as well when fitted separately to the naturalistic data and the simulator study data. A potential reason for this difference in performance could be that the data sets contained data with different criticality levels in terms of relative yaw angle at steering initiation. The simulator data angles were greater than 2°, and the naturalistic data sets angles were mostly below 1.5°. To achieve a good fit over the entire investigated relative yaw angle range, a threshold model turned out to be a reasonable alternative to the polynomial model. The threshold model featured a linear relationship with the change in splay error for low relative yaw angles (<1.5°), and a linear relationship with the relative yaw angle itself for higher angles. The slightly better R^{-2} value ($R^{-2} = 0.85$) for this model, compared to the polynomial model, may however not compensate for the increased model complexity (five parameters instead of three).

A correlation analysis showed that the splay angle and relative yaw angle are closely correlated (see Appendix D). This correlation implies that the low range of relative yaw angles could be explained by a linear relation to the relative yaw angle with results similar to those obtained by using the change in splay error risk metric. To confirm this, a piecewise linear function of the relative yaw angle, with a breakpoint at 1.5°, was fitted to the data (see Appendix E). The resulting R^{-2} value was 0.85, in accordance with the R^{-2} value in the original, change-in-splay-error-based threshold model. More importantly, the model coefficient values were very close to the coefficients obtained by a linear approximation of the polynomial, yaw-angle-based model in the high (approximated around 2.7°) and low (approximated around 0.7°) range, respectively. Thus, the threshold model could be considered a (piecewise) linearized version of the previously suggested polynomial model. Since both the threshold and polynomial models suggested in this study have high performances, more studies would be necessary to understand whether observed the steering amplitudes are the results of a continuous (polynomial) process, or rather should be understood as resulting from separate processes depending on the situation kinematics (relative yaw angle).

In spite of how well a relative yaw angle-based model estimates the change in relative yaw rate, it is not reasonable to believe that

drivers decide to steer solely based on this information in all kinds of kinematic situations: drivers must also use some measure of criticality related to estimated departure time or distance. Otherwise, drivers would always react in the same way to relative yaw angle deviations regardless of the vehicle's lateral lane position (i.e., even when driving close to the lane marker on the opposite side of the road).

The performances of the models fitted to the naturalistic data sets were influenced mainly by the change in splay error, in contrast to the performances of the models simultaneously fitted to all data sets (or solely to the simulator study data), which were dominated by the relative yaw angle predictor. Whether this difference is caused by the difference in event severity levels or the different driving conditions (i.e., naturalistic driving or driving in a simulator), this observation may be essential for the practical applications of the models. Simulations of low-severity lane departures, such as most of the events in the naturalistic data sets, could benefit from using a change-in-splay-error-based model, while virtual tests with high-severity events may require other or additional predictors (such as the relative yaw angle). Though the threshold model presented in this study have a high performance on the considered data sets, more research would be necessary to confirm which model type (change in splay error-based or relative yaw angle-based) would be appropriate for which situation (or level of criticality).

4.3. Identification and accuracy of the primary corrective steering adjustments

Validation of the identified primary corrective steering adjustments at a subjective level was conducted by manually inspecting the "intuitive" location of steering initiation. However, this step was non-trivial, particularly for the naturalistic driving data sets. In some cases, the total recovery maneuver consisted of several steering adjustments (as exemplified in the lower panel of Fig. 3 in Section 2.2.2); sometimes there was no way to judge which adjustment was "primary". In other cases, the primary corrective steering adjustment could not be distinguished from ordinary steering adjustments made at almost the same time. Hence, a small sensitivity analysis was performed on the events in the SHRP2 data set to study the impact of choosing alternative steering adjustments. The results showed that the conclusions drawn in this paper were robust to this variation.

4.4. Implications of differences in data set characteristics

This work was based on combining data from three different data sets and using these data to draw conclusions about the behavior of a generic driver. While using several different data sources may contribute to the strength and generalizability of the results, it also raises questions about data comparability and, consequently, the validity of the performed analyses.

Data set differences were already obvious in the selection of lane departure events and the data preprocessing step, discussed in Sections 2.1–2.2. Since the data were collected using different kinds of equipment and in different environments, the preprocessing had to be individually tailored to each data set. Different thresholds for steering adjustment extraction were used to make the final data sets comparable. In particular, a relatively high threshold was applied to the data from the simulator study. This was necessary to avoid identifying the artificially applied yaw angle deviation as part of the primary steering adjustment. The threshold choice was motivated by the relatively severe primary corrective steering adjustments in this data set and, thus, did not induce any limitations in the subsequent analysis.

A few noteworthy differences were also observed in the methods used to record glance behavior, and in the definitions of on–/off-road glances (see Section 2.2). These differences may have impacted the steering initiation distributions (see Section 3). Nonetheless, the influence of the methodological differences in the collection and processing of glance data between data sets is arguably not substantial (all underlying studies aimed to capture the current glance direction, but had different means of achieving that objective), and the conclusion that drivers can initiate corrective steering using peripheral vision still holds.

Moreover, the Run-off-road simulator study data set differed from the naturalistic driving data sets in several ways, apart from being based on data from a controlled test in a virtual environment. The most obvious difference was that all drivers were performing a non-driving-related, visual-manual secondary task at the start of the lane departure event. This task required the driver to keep a finger on a display. Consequently, the driver could only hold the steering wheel with one hand while looking off-road. This constraint (one-handed driving) may have delayed the motor reaction or influenced the steering amplitude. More research is needed to confirm whether one-handed driving generally causes response delays. The simulator study by Ameyoe and colleagues (Ameyoe et al., 2015), which aimed to assess driver distraction, is one of very few studies explicitly addressing one-handed driving. However, they did not find any significant differences in driving performance (standard deviation of lateral position and steering wheel reversal rate) between the one-handed driving condition and baseline driving.

Furthermore, the drivers in the simulator study were aware of being participants in an experiment and that they were being closely monitored, which may potentially have increased their vigilance. However, the distraction task successfully induced longer glances away from the road, than those that naturally occurred when driving freely (without performing a task). Nonetheless, two of the drivers showed a gaze-shifting behavior between the distraction task and the road ahead. However, they looked back to the road only once (check glance). Their response patterns did, however, not qualitatively differ from the general response pattern observed for the other drivers.

The participant selection also differed between the data collection studies. Particularly, the EyesOnRoad data set consisted of drivers who were (or were closely related to) Volvo cars employees. Though the participants did not risk any repercussions from their employer for, for example, inappropriate driving behavior or violating traffic laws, this relation may still have imposed some bias in the collected data. For example, it is reasonable to believe that the participants had more detailed knowledge about the vehicle and its functions than an average driver would have had. The influence of this knowledge is presumably negligible in this study, since drivers'

Table A1
Summary of the database query and the number of remaining events following each step.

Query condition	Event inclusion criteria ("or")	Remaining number of events
Subject vehicle configuration	Drive off-road to the right (1)Drive off-road to the left (2)	1056
Event severity	Crash Near-crash	1055
Surface condition	Dry Wet	1043
Pre-incident maneuver	Going straight, constant speed Going straight, accelerating Going straight, but with unintentional "drifting" within lane or across lanes Decelerating in traffic lane Negotiating a curve	301
Relation to junction	Non-junction Intersection-related Entrance/Exit ramp Interchange area Driveway, alley access, etc.	200
Intersection influence	Yes, interchange No	165
Construction zone	Not construction zone-related	158
Infrastructure	None	156
Driver impairments	None apparent Angry Other emotional state Restricted to wheelchair Impaired due to previous injury Deaf	126

Table A2
Summary of the manual filtering process and the number of remaining events following each step.

Evaluated condition	Event inclusion criteria ("or")	Remaining number of events
Low speed	Speed at departure $>$ 50 km/h	36
Manual judgement of vid***eo or final narratives	No excessive speeding No turning No apparent influence from other road users (e.g., being blocked by other cars) Not environment or weather-related (e.g., sun glare) Only straight driving intent (e.g., no lane change preparation)	26
Speed data	Available	11
GPS data	Available	6

Table C1
The correlation matrix for the model predictors.

$iTLC_m$	0.3	0.24	0.37
	$\dot{S}_{err}$	0.75	0.87
		$r_{c,1.5}$	0.82
			θ

emergency responses are typically reflexive and performed in open loop (Markkula et al., 2014; Markkula, 2015).

To summarize, the data set differences can be considered as additional "noise" in the analyzed data. All analyses in this paper reach the same (high-level) conclusions regardless of data set studied, except for the conclusions on the best-fitting steering amplitude model (since the data sets are best described by different models). Therefore, the results presented here can be considered more robust and generalizable than if the analyses had been performed on a single, homogeneous data set.

4.5. Limitations and future work

Although most limitations in the current work have already been discussed, there are some additional remarks:

First, the analyses in this paper are restricted to unintentional lane departure drift events on straight roads, with the primary causation mechanism being driver distraction or inattention. In addition, all data were collected on European (Swedish) or US roads. The conclusions may thus be invalid for events with vastly different causation mechanisms or in other geocultural areas.

Table C2
R^{-2} values and upper and lower limits of the 95 % HPD interval for all model candidates fitted to all data sets. The best-performing models are marked with bold R^{-2} values. An empty cell means the predictor was not considered for the current candidate model (row).

Model ($\ddot{\theta}$ ⋯)	$\mathbf{R^{-2}}$	**Mean 95 % HPD interval** (***upper***: low; ***lower***: high)				
		$iTLC_m$	$r_{c,1.5}$	$\dot{S}_{err}$	θ	θ^2
	0.16	−19.61				
$iTLC_m$		−15.84				
$\dot{S}_{err}$	0.66			−0.76		
				−0.7		
$r_{c,1.5}$	0.65		−7.09			
			−6.53			
θ	**0.75**				−12.82	
					−11.94	
$\theta + iTLC_m$	0.74	−4.30			−12.45	
		−1.47			−11.49	
$\theta + \theta^2$(orthogonal*)	**0.84**				−79.76	−29.69
					−75.72	−25.65

* See Section 3.2.4.

Table C3
R^{-2} values and upper and lower limits of the 95 % HPD interval for all model candidates fitted to the naturalistic data sets only. The best-performing model is marked with a bold R^{-2} value. An empty cell means the predictor was not considered for the current candidate model (row).

Model ($\ddot{\theta}$ ⋯)	$\mathbf{R^{-2}}$	**Mean 95 % HPD interval** (***upper***: low; ***lower***: high)					
		$iTLC_m$	$r_{c,1.5}$	$\dot{S}_{err}$	$\dot{S}_{err}{}^2$	θ	θ^2
	−0.01	−4.33					
$iTLC_m$		0.81					
$\dot{S}_{err}$	0.33			−0.20			
				−0.10			
$r_{c,1.5}$	0.12		−1,49				
			−0.50				
θ	0.14					−2.75	
						−0.97	
$\dot{S}_{err} + iTLC_m$	0.32	−4.16		−0.20			
		0.94		−0.10			
$\dot{S}_{err} + \dot{S}^2_{err}$(orthogonal*)	0.34			−8.1–4.14	−3.69		
					0.26		
Best model from Section C.1	0.13					−6.18	−0.73
$\theta + \theta^2$(orthogonal*)						−2.21	3.23

* See Section 3.2.4.

Table C4
R^{-2} values, and upper and lower limits of the 95 % HPD interval for all model candidates fitted to only the simulator study data set only. The best-performing model is marked with a bold R^{-2} value. An empty cell means the predictor was not considered for the current candidate model (row).

Model ($\ddot{\theta}$ ⋯)	$\mathbf{R^{-2}}$	**Mean 95 % HPD interval** (***upper***: low; ***lower***: high)				
		$iTLC_m$	$r_{c,1.5}$	$\dot{S}_{err}$	θ	θ^2
	−0.03	−7.99				
$iTLC_m$		−4.97				
$\dot{S}_{err}$	0.21			−0.57		
				−0.46		
$r_{c,1.5}$	0.19		−4.94			
			−3.96			
θ	**0.44**				−7.99	
					−4.97	
$\theta + iTLC_m$	0.38	−0.64			−26.68	
		−2.27			−22.7	
$\theta + \theta^2$(orthogonal*)	**0**.38				−38.84	−4.75
					−29.99	0.12

* See Section 3.2.4.

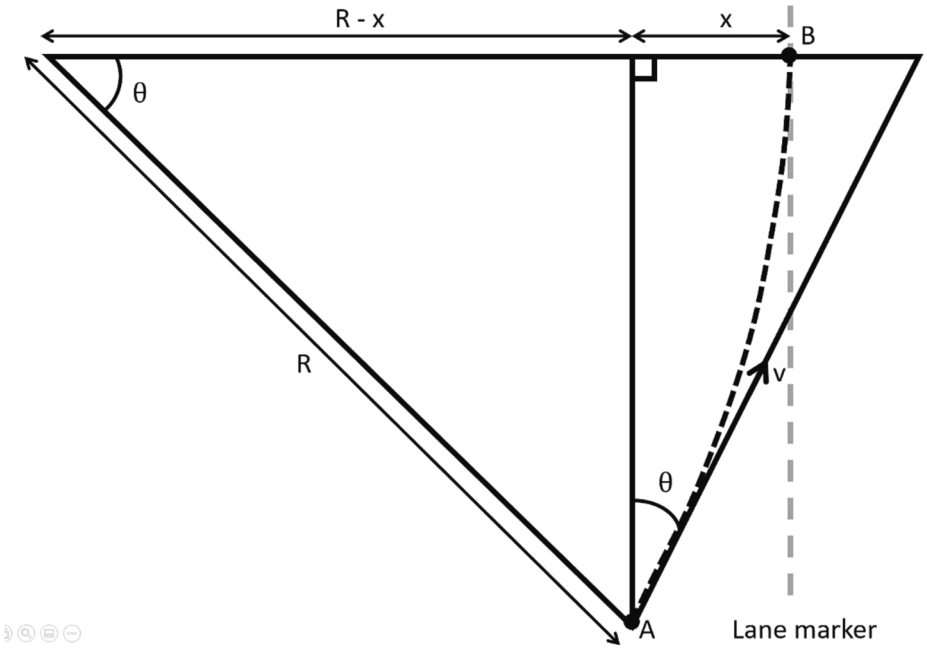

Fig. D1. A schematic illustration of the yaw rate required to bring the vehicle back into the lane at point B. The vehicle is positioned at point A and drives toward the lane marker at speed v with relative yaw angle θ.

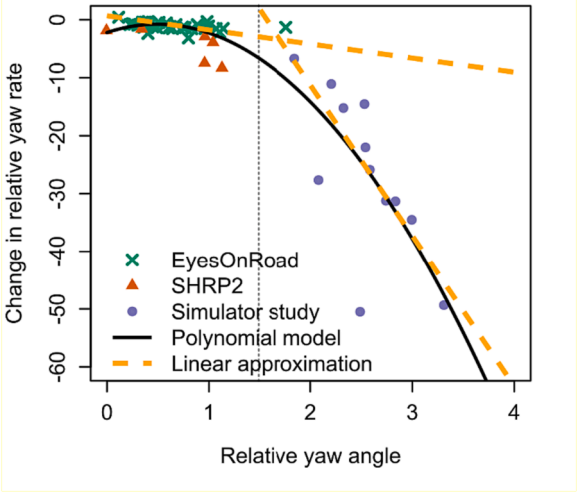

Fig. E1. The relative yaw angle risk metric plotted against the change in relative yaw rate (colored markers). The best polynomial model fitted to all data sets is shown with a solid black line, and its linear approximations are shown with dashed orange lines. A gray dotted line marks the border between the low and high relative yaw angle ranges (i.e., the threshold value). (For interpretation of the references to colour in this figure legend, the reader is referred to the web version of this article.)

Second, the complete data set comprised only 52 lane departure events, which could be considered a low number of data points for drawing firm conclusions. However, since detailed recordings of critical lane departures are rare, only few such events can be found in a single data set. The low number of events in each data set was one of the motivations for performing a joint analysis on all available data sets (treating them as a single collection of lane departure events). The number of events (six) was particularly scant for the SHRP2 data set. However, these departures were more severe (in terms of crash risk) than those observed in the other naturalistic data set (the EyesOnRoad data set). Thus, including these few events contributed to a more comprehensive analysis of naturalistic lane departures. The fact that we do include several data sets from different data sources should help making the results more generalizable than if we

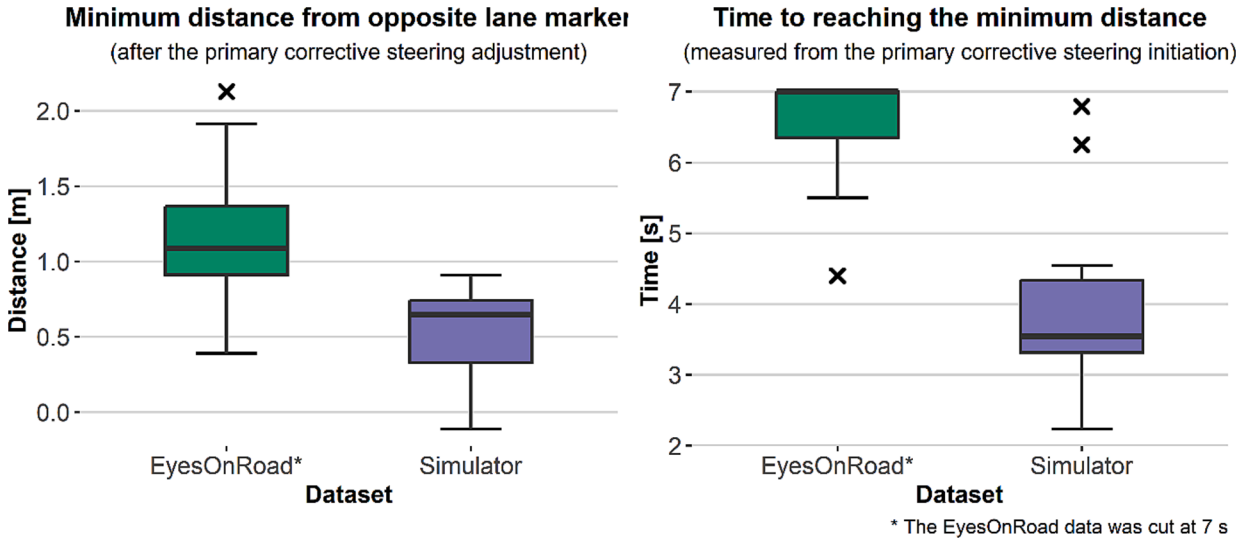

Fig. F1. *Left panel*: A comparison of the minimum distance (in meters) to the opposite lane marker after the primary corrective steering maneuver for the EyesOnRoad data set (green) and Run-off-road simulator study data sets (purple). *Right panel*: A comparison of the time duration before reaching the minimum distance to the opposite lane marker for the EyesOnRoad (green) and Run-off-road simulator study (purple) data sets. (For interpretation of the references to colour in this figure legend, the reader is referred to the web version of this article.)

only included a single data set from a single study.

Additionally, only 21 different drivers were responsible for the 52 lane departure events. The highest number of different drivers are found in the simulator data set, but, in contrast to the other data sets, these drivers were driving in a very controlled environment and were exposed to the exact same experiment setup. Thus, the simulator data set contributes with a larger variation in driver characteristics, while the EyesOnRoad data set contributes with a larger variation in scenario characteristics. Both these variables are important, but we catch only both when studying the combined data sets. To ensure that the conclusions drawn in the current analyses are representative of general driver behavior, future studies involving a high number of drivers representative of the targeted population (or geocultural area) are necessary.

Although this work focused on the primary corrective steering adjustment, adding subsequent steering adjustments in the analysis could enable a more comprehensive understanding of driverś lane departure recovery maneuvers, as well as an assessment of how the complete maneuvers may differ between the data sets. Appendix E demonstrates that there is a significant difference in the severity of the recovery maneuvers between the naturalistic and driving simulator study data sets. The severity was quantified in terms of the minimum distance to the opposite lane marker (after corrective steering initiation) and the duration of the maneuver before reaching that minimum distance.

The events studied in this paper were all critical (although to different degrees), and all drivers started steering relatively close to the lane departure; thus, it may not have been possible, or necessary, to capture human steering behavior related to criticality (in time or distance) with the current modeling paradigm. More data, preferably from controlled studies, are required to analyze the drivers' use of visual risk metrics in more detail, potentially including other lane departure risk metrics (or combinations) that were not studied here. For example, as mentioned, it has been suggested that drivers may use optic flow information and target waypoints to guide steering (Kountouriotis et al., 2016; Lappi et al., 2020; Mole et al., 2016, 2019; Okafuji et al., 2018; Tuhkanen et al., 2019; Wilkie & Wann, 2003). Performing future analyses with a larger number of (high quality) data points available, other risk metrics may turn out to be important, and thus, the models suggested in this paper may need to be revisited.

With more data and knowledge about how drivers use visually available lane departure risk metrics, it would be possible to proceed from the linear models devised in this paper to more advanced modeling frameworks. Markkula et al. (2018) used a noisy evidence accumulation framework based on sensory predictions in combination with the two-point model for steering suggested by Salvucci and Grey (Salvucci & Gray, 2004) to model non-critical lane keeping. Since the framework has also been used to model critical situations in the longitudinal domain (Svärd et al., 2017, 2021), it should be possible to apply it to critical lane departures as well.

Glance behavior will be an essential part of accurate models for critical lane departures caused by distraction. Though drivers may be able to acquire visual input through the peripheral visual system during off-road glances, some visual cues may be substantially degraded. This could potentially be addressed in the steering models in a similar manner as in the partial looming perception approach for brake response models introduced by Svärd et al. (2021).

5. Conclusions

Drivers' primary corrective steering adjustments when the vehicle is drifting out of the lane on straight roads were investigated using naturalistic and simulated driving data from three sources. It was observed that visually distracted drivers typically initiate their

primary corrective steering adjustment before, or at the same time as, looking up toward the road ahead. A possible explanation for this behavior, which aligns with previous research on non-critical lane-keeping behavior, is that drivers use peripheral vision to guide their corrective actions in critical lane departures (Summala et al., 1996).

Contrary to expectations, a polynomial model of the relative yaw angle measured at the initiation of the primary corrective steering adjustment showed good performance in predicting the adjustment amplitude. This model outperformed models based on higher-complexity risk metrics such as splay angle, critical yaw rate, and modified iTLC, despite the high variability in data set characteristics (in terms of both data collection methods and the event severity levels). However, change in splay error explained the steering amplitudes in naturalistic data better than the relative yaw angle. The best model fit was achieved by combining the change in splay error and relative yaw angle metrics into a threshold model. In this way, the change in splay error was used to explain the less-critical data points (corresponding to low relative yaw angles), and the relative yaw angle could explain the data points at higher angles. Since an urgency component (estimated time or distance to departure) is lacking in the relative yaw angle-based models, more research is recommended to fully understand and model the driver's recovery behavior in critical lane departure situations.

Computational models of driver's recovery maneuvers in lane departure events will be essential for realistic virtual in-vehicle system assessments targeting lateral advanced driver assistance systems such as emergency LKAS. The models may also be beneficial when evaluating the safety benefits and driver acceptance of automated driving systems.

Declaration of competing interest

The authors declare the following financial interests/personal relationships which may be considered as potential competing interests: The authors all have relationships to Volvo Car Corporation as follows: Malin Svärd and Mikael Ljung Aust: employees; Jonas Bärgman: adjunct professor; Gustav Markkula: consulting advisor.

Data availability

The authors do not have permission to share data.

Acknowledgments

This research was funded by FFI Vinnova, the Swedish governmental agency for innovation, as part of the project Improved Quantitative DRIver behavior models and Safety assessment methods for ADAS and AS (QUADRIS: nr. 2020-05156). Gustav Markkula received funding from the UK Engineering and Physical Sciences Research Council, grant EP/S005056/1.

The Run-off-road simulator study data set used in this study was collected by the Swedish National Road and Transport Research Institute (VTI), funded by the Swedish excellence centre Virtual Prototyping and Assessment by Simulation (ViP) and VINNOVA as part of the ELKA and QUADRAE projects. The authors wish to thank Alexander Eriksson, Bruno Augusto, Niklas Strand, and Jesper Sandin for the design and execution of the experiment and for making the data available for this study.

The SHRP2 data set was provided by the Virginia Tech Transportation Institute (VTTI) under a Data License Agreement (DUL: SHRP2-DUL-16-172; DOI:s: 10.15787/VTT1/WX2KSK, 10.15787/VTT1/OIQDNQ, and 10.15787/VTT1/FQLUWZ). The findings and conclusions of this paper are those of the authors and do not necessarily represent the views of VTTI, the Transportation Research Board (TRB), or the National Academies.

The authors also want to acknowledge all people involved in the EyesOnRoad FOT data collection.

Last, but not least, thanks to Pierluigi Olleja for providing the code base for the GPS-matching step in the yaw rate calculation for the naturalistic data sets (see Appendix B); to Kristina Mayberry for the language review; and to Carol Flannagan for reviewing the statistical concepts used in this study.

Appendix A. – The data selection process for the SHRP2 data set

The original set of lane departure events in the SHRP2 data set was reduced in two steps to include only those events relevant to the current use case. The first step consisted of a database query, which reduced the data set from 1056 to 126 events; see Table A1. In the second step, all 126 events were manually examined, and the data set was further reduced to only 6 events. Details of the process in the second step are given in Table A2.

Appendix B. – Relative yaw rate calculation in the naturalistic data sets

The vehicles in the naturalistic data sets were instrumented with a yaw rate sensor, whose data could be fused with the GPS coordinates to calculate the relative yaw angle of the vehicle as follows.

First, the yaw rate signal was filtered, integrated, and offset-adjusted to match the GPS coordinates surrounding the event. This step was realized through an optimization procedure that minimized the distance error between the actual GPS coordinates and the coordinates estimated using the integrated and offset-adjusted yaw rate. To avoid optimizing against the lane departure, time samples with a lateral distance from the vehicle center to the lane marker less than 1.2 m were excluded.

Next, the relative yaw angle was calculated by subtracting the road heading angle (calculated from the GPS coordinates) from the optimized yaw angle. This signal could then be numerically differentiated to obtain the relative yaw rate and change in relative yaw

rate which were used as steering signals in this paper.

Appendix C. – Model selection

Here, the model selection process is presented in detail when applied to (1) all data sets simultaneously, (2) naturalistic data sets only, and (3) only the simulator study data set.

The model selection process was based on forward predictor elimination. The considered predictors were: modified iTLC ($iTLC_m$), critical yaw rate at 1.5 s ($r_{c,1.5}$), change in splay error ($\dot{S}_{err}$), and relative yaw angle (θ). A correlation analysis between the predictors showed high correlation between the three last mentioned predictors, see Table C1, thus no models including combinations of these were studied. The output of each model was the change in relative yaw rate ($\ddot{\theta}$).

C.1 Model selection based on all data sets

Table C2 provides an overview of the investigated models, their respective R^{-2} values, and the 2.5 and 97.5 percentiles of the posterior HPD intervals for each included predictor. For the combination of all data sets, we observed a dominance of the relative yaw angle predictor. Therefore, we also investigated whether a higher degree polynomial (a cubic predictor) could further improve the model, by adding a polynomial predictor: θ^2. To avoid predictor correlation, the polynomial predictor was transformed to be orthogonal to θ (see Section 3.2.4). In this way, a comparison between models based on more complex metrics only and models dominated by the simple yaw angle metric was possible.

C.2 Model selection based on the naturalistic data sets

The model selection process based on the naturalistic data sets alone was equivalent to the process performed on all data sets (see Section C.1). The models which performed best on the complete data set (including data from the simulator study) were also evaluated using only the naturalistic data sets. The results are presented in Table C3.

Note that no relative yaw angle predictor dominance was observed for the naturalistic data set models. Instead, for these data sets, the change in splay error predictor seemed to dominate the models. A cubic relationship was thus investigated by adding a polynomial factor $\dot{S}_{err}{}^2$.

C.3 Model selection based on the simulator study data set

The model selection process based only on the simulator data set was equivalent to the process performed on all data sets (see Section C.1). The results are presented in Table C4. No single predictor was found to clearly dominate in this data set.

Appendix D. – Theoretical derivation of required steering amplitude

In Equations D.1 to D.4, the precise steering amplitude (i.e., change in yaw rate, $\ddot{\theta}$) required to bring the vehicle back into the lane is derived; see Fig. D1 for the notation used.

$$\Leftrightarrow \frac{R-x}{R} = \cos\theta$$

$$\Leftrightarrow R - x = R\cos\theta$$

$$\Leftrightarrow R(1-\cos\theta) = x$$

$$\Leftrightarrow R = \frac{x}{1-\cos\theta} \tag{D.1}$$

Relation between the radius R and the yaw rate $\dot{\theta}$:

$$\dot{\theta} = \frac{v}{R} \tag{D.2}$$

$$(\text{D.1}) \text{ and } (\text{D.2}) \Rightarrow \dot{\theta} = \frac{v}{x}(1-\cos\theta) \tag{D.3}$$

$$Taylorexpansion \Rightarrow \dot{\theta} = \frac{v}{x}(1-(1-\theta^2)$$

$$\Leftrightarrow \dot{\theta} = \frac{v}{x}\theta^2 \tag{D.4}$$

Assuming an initial relative yaw rate close to zero, the required change in yaw rate will be proportional to θ^2, as shown by Equation

D.4.

Appendix E. – Relation between a threshold model and the polynomial model

To investigate the performance of a threshold model entirely based on the relative yaw angle risk metrics, we set up the following model:

$$\ddot{\boldsymbol{\theta}} = \begin{cases} \boldsymbol{\beta}_0 + \boldsymbol{\beta}_1\theta, \theta < 1.5^{\circ} \\ \boldsymbol{\beta}_2 + \boldsymbol{\beta}_3\theta, \theta \geq 1.5^{\circ} \end{cases} \tag{E.1}$$

The model was fit to the combination of all data sets. The model performance (overall $R^{-}2 = 0.85$) was equal to the performance of the threshold model suggested in Section 3.2.5. The optimal parameter set was: $\beta_0 = 0.04$, $\beta_1 = -2.57$, $\beta_2 = 40.37$, and $\beta_3 = -26.24$. The model coefficients were found to very closely match the values obtained by linearizing the polynomial model suggested in Section 3.2.4 in the low and high yaw angle range, respectively. Specifically, we performed a linear approximation around $\theta_0 = 0.7^{\circ}$ and $\theta_0 = 2.7^{\circ}$. Eq. E.2-E.7 show the derivation of the linear coefficients:

$$f(\theta) = \gamma_0 + \gamma_1\theta + \gamma_2\theta^2 \tag{E.2}$$

$$f'(\theta) = \gamma_1 + 2\gamma\theta \tag{E.3}$$

Linearizing around θ_0 :

$$f(\theta) \approx f(\theta_0) + f'(\theta_0)(\theta - \theta_0) \tag{E.4}$$

$$\Leftrightarrow$$

$$f(\theta) \approx (\gamma_1 + 2\gamma_3\theta_0)\theta + \gamma_0 - \gamma_3\theta_0^2 \tag{E.5}$$

$$\Rightarrow$$

$$k = \gamma_1 + 2\gamma_3\theta_0 \tag{E.6}$$

$$m = \gamma_0 - \gamma_3\theta_0^2, \tag{E.7}$$

where k is the slope and m the intercept of the linear approximation. Inserting $\theta_0 = 0.7^{\circ}$, $\theta_0 = 2.7^{\circ}$, and using the coefficient values from the polynomial model Section 3.2.4 in Eq. (E.2) yields m = 0.68 and k = -2.43 in the lower relative yaw angle range, and m = 40.82 and k = -26.04 in the high relative yaw angle range. Fig. E1 illustrates the linear approximations on top of the polynomial function:

Appendix F. – Differences in total corrective steering maneuver execution

A lane departure recovery maneuver may consist of several discrete steering adjustments after the primary corrective steering adjustment before reaching the desired lateral lane position. The drivers' *total corrective steering maneuvers*—which consisted of the primary corrective steering adjustment and possible additional steering adjustments in the same direction—were studied to obtain a holistic view of drivers' recoveries from unintentional lane departures and how these differ between the data sets. The total corrective steering maneuver was defined as starting at the initiation of the primary corrective steering adjustment and ending when the minimum lateral distance to the opposite lane marker was reached.

The analysis was performed on the events from the EyesOnRoad and Run-off-road simulator data sets. It did not include any events from the SHRP2 data set since the data available ended before the maneuvers were complete. In addition, several events in the EyesOnRoad data set had not reached the minimum distance to the opposite lane markers 7 s after initiating the recovery maneuver, which was the end time of the available data set. The minimum distance was measured at the last time sample for these events.

It was observed that the total corrective steering maneuvers had higher amplitudes and were briefer in the (less critical) events from the EyesOnRoad naturalistic data set than in the substantially more critical events from the simulator study; see Fig. F1. The differences were compared through two-sample *t*-tests. The results confirmed significant differences in both execution times and minimum distances to the opposite lane marker ($p < 0.0001$).

One possible explanation for the observed maneuvering differences is the origin of the data. Drivers may not show the same driving characteristics in a driving simulator as on a real road (see, e.g., the review by Wynne et al., 2019). The differences may be particularly marked during steering interventions, since realistic steering feedback is difficult to achieve in a driving simulator (Mircea, 2019). However, routine lane-keeping in a driving simulator has been shown to have good behavioral validity (H. C. Lee et al., 2003). Moreover, the current study was performed in a very advanced driving simulator for which drivers' responses to unexpected steering interventions have been validated toward drivers' responses in corresponding situations when driving a real vehicle on a test track (Jansson et al., 2014). Thus, it is improbable that the simulator environment entirely explains the observed differences between the data sets.

Another way to explain the maneuver differences could be the severity level of the included events in each data set. The EyesOnRoad data set consists of low-severity incidents in everyday driving which the drivers successfully resolved. The relatively low criticality level is further confirmed by the low values (compared to the simulator data set) of most lane departure risk metrics (shown in Fig. 11 in Section 3.2.1). In contrast, all lane departures in the simulator data set could be considered sudden, highly critical, and unexpected.

Markkula and colleagues (Markkula, 2015; Markkula et al., 2014) state that evasive maneuvers in critical situations tend to have open-loop characteristics, while routine driving maneuvers are performed in closed-loop. Open-loop steering could explain the tendency toward rapid reactions in which the driver steers more than necessary, as observed in the simulator data. These maneuvers were characterized by lateral overshoot; some drivers even exited the lane on the opposite side of the road before regaining control. Similarly, the closed-loop paradigm would explain the longer duration of the maneuvers in the less critical events from the EyesOnRoad data set.

References

Alvarez, S., Page, Y., Sander, U., Fahrenkrog, F., Helmer, T., Jung, O., Hermitte, T., Düering, M., Döering, S., & Op den Camp, O. (2017). Prospective effectiveness assessment of ADAS and active safety systems via virtual simulation: A review of the current practices. *25th Int. Tech. Conf. on the Enhanc. Saf. of Veh. (ESV)*.

Amarasingha, N., & Dissanayake, S. (2014). Factors associated with rural run-off-road and urban run-off-road crashes: a study in the United States. *J. of Soc. for Transp. and Traffic Stud., 5*(4), 39–51. https://doi.org/10.31705/apte.2014.14

Ameyoe, A., Mars, F., Chevrel, P., Le-carpentier, E., & Illy, H. (2015). Estimation of driver distraction using the prediction error of a cybernetic driver model. *Proc. of the Driv Simulator Conf. Eur., 2015*, 13–18.

Beall, A. C., & Loomis, J. M. (1996). Visual control of steering without course information. *Percept., 25*(4), 481–494. https://doi.org/10.1068/p250481

Benderius, O., & Markkula, G. (2014). Evidence for a fundamental property of steering. *Proc. of the Hum Factors and Ergon. Soc. Annu. Meet., 58*(1), 884–888. https://doi.org/10.1177/1541931214581186

Boer, E. R. (2016). Satisficing curve negotiation: explaining drivers' situated lateral position variability. *IFAC-PapersOnLine, 49*(19), 183–188. https://doi.org/10.1016/j.ifacol.2016.10.483

Calvert, E. S. (1954). Visual Judgments in Motion. *J. of Navig., 7*(3), 233–251. https://doi.org/10.1017/S0373463300020907

Cao, J., Lu, H., Guo, K., & Zhang, J. (2013). A driver modeling based on the preview-follower theory and the jerky dynamics. *Math. Probl. Eng., 2013*. https://doi.org/10.1155/2013/952106

Cheng, S., Song, J., & Fang, S. (2020). A universal control scheme of human-like steering in multiple driving scenarios. *IEEE Trans. on Intell. Transp. Sys., 22*(5), 1–11. https://doi.org/10.1109/tits.2020.2982002

Cicchino, J. B., & Zuby, D. S. (2017). Prevalence of driver physical factors leading to unintentional lane departure crashes. *Traffic Inj. Prev., 18*(5), 481–487. https://doi.org/10.1080/15389588.2016.1247446

Donges, E. (1978). A two-level model of driver steering behavior. *Hum. Factors: The J. of Hum. Factors and Ergon Soc., 20*(6), 691–707. https://doi.org/10.1177/001872087802000607

Eriksson, A., Augusto, B., Strand, N., & Sandin, J. (2018). Drivers ' recovery performance in a critical run-off-road scenario – A driving simulator study. *Proc. of the 6th Humanist Conf*.

Gelman, A., Carlin, J. B., Stern, H. S., Dunson, D. B., Vehtari, A., & Rubin, D. B. (2013). *Bayesian Data Analysis* ((3rd ed.).). Chapman & Hall / CRC Press.

Godthelp, H. (1988). The limits of path error-neglecting in straight lane driving. *Ergon., 31*(4), 609–619. https://doi.org/10.1080/00140138808966703

Goodridge, C. M., Mole, C. D., Billington, J., Markkula, G., & Wilkie, R. M. (2022). Steering is initiated based on error accumulation. *J. of Exp. Psychol.: Hum. Percept. Perform., 48*(1), 64–76. https://doi.org/10.1037/xhp0000970

Gordon, T., Blankespoor, A., Barnes, M., Blower, D., Green, P., & Kostyniuk, L. (2009). Yaw rate error – a dynamic measure of lane keeping control performance for the retrospective analysis of naturalistic driving data. *Int. Tech. Conf. on the Enhanc. Saf. of Veh., ESV*, 1–10.

Gordon, T., & Srinivasan, K. (2014). Modeling human lane keeping control in highway driving with validation by naturalistic data. *Conf. Proc.-IEEE Int. Conf. on Sys., Man and Cybern.*, 2507–2512. https://doi.org/10.1109/smc.2014.6974303

Hallmark, S. L., Oneyear, N., Tyner, S., Wang, B., Carney, C., & McGehee, D. (2014). Analysis of Naturalistic Driving Study Data: Roadway Departures on Rural Two-Lane Curves. *In SHRP2 Report S2–S08D-RW-1*.

Hankey, J. M., Perez, M. A., & McClafferty, J. A. (2016). Description of the SHRP 2 naturalistic database and the crash, near-crash, and baseline data sets. [Report].

Hastie, T., Tibshirani, R., Friedman, J., 2009. Kernel smoothing methods. The Elements of Statistical Learning: Data Mining, Inference, and Prediction, 191-218.

Hildreth, E. C., Boer, E. R., Beusmans, J. M. H., & Royden, C. S. (2000). From vision to action: Experiments and models of steering control during driving. *J. of Exp. Psychol.: Hum. Percept. Perform., 26*(3), 1106–1132. https://doi.org/10.1037/0096-1523.26.3.1106

Horrey, W. J., Lesch, M. F., & Garabet, A. (2008). Assessing the awareness of performance decrements in distracted drivers. *Accid. Anal. & Prev., 40*(2), 675–682. https://doi.org/10.1016/j.aap.2007.09.004

International Organization for Standardization. (2019). Road vehicles — Prospective safety performance assessment of pre- crash technology by virtual simulation — Part 1: State-of-the-art and general method overview (ISO/TR 21934-1:2021).

Isaksson-Hellman, I., & Lindman, M. (2018). Traffic safety benefit of a lane departure warning system. *Int. J. of Automot. Eng., 9*(4), 289–295. https://doi.org/10.20485/JSAEIJAE.9.4_289

JAGS. (n.d.). https://mcmc-jags.sourceforge.io/.

James, G., Witten, D., Hastie, T., & Tibshirani, R. (2017). An Introduction to Statistical Learning with Applications in R. In G. Casella, S. Fienberg, & I. Olkin (Eds.), *Springer Texts in Statistics*. Springer.

Jansson, J., Sandin, J., Augusto, B., Fischer, M., Blissing, B., & Källgren, L. (2014). Design and Performance of the VTI Sim IV. *Proc. of the Driv. Simul. Conf. 2014*, 4.1-4.7.

Karlsson, J., Apoy, C., Lind, H., Dombrovskis, S., Axestål, M., & Johansson, M. (2016). *EyesOnRoad An anti-distraction Field Operational Test*. [Report.

Kiefer, R. J., LeBlanc, D. J., & Flannagan, C. A. (2005). Developing an inverse time-to-collision crash alert timing approach based on drivers' last-second braking and steering judgments. *Accid. Anal. & Prev., 37*(2), 295–303. https://doi.org/10.1016/j.aap.2004.09.003

Koch, K.-R. (2007). *Introduction to Bayesian statistics* (2nd ed.). Springer Berlin, Heidelberg. https://doi.org/10.1007/978-3-540-72726-2.

Kondo, M., & Ajimine, A. (1968). Driver's Sight Point and Dynamics of the Driver-Vehicle-System Related to It. *Automot. Eng. Congr. & Expo*.

Kondoh, T., Furuyama, N., Hirose, T., & Sawada, T. (2014). Direct Evidence of the Inverse of TTC Hypothesis for Driver's Perception in Car-Closing Situations. *Int. J. of Automot. Eng., 5*(4), 121–128. https://doi.org/10.20485/jsaeijae.5.4_121

Kountouriotis, G. K., & Merat, N. (2016). Leading to distraction: Driver distraction, lead car, and road environment. *Accid. Anal. & Prev., 89*, 22–30. https://doi.org/10.1016/j.aap.2015.12.027

Kountouriotis, G. K., Mole, C. D., Merat, N., & Wilkie, R. M. (2016). The need for speed: Global optic flow speed influences steering. *R. Soc. Open Sci., 3*(5). https://doi.org/10.1098/rsos.160096

Kuehn, M., Hummel, T., & Bende, J. (2009). Benefit Estimation of Advanced Driver Assistance Systems for Cars Derived from Real-life Accidents. *Proc. of the 21st Int. Tech. Conf. of Th Enhanc. Saf. of Veh. Conf. (ESV), Stuttgart, Germany, June 15-18*, 1–10.
Kusano, K. D., & Gabler, H. C. (2014). Comprehensive Target Populations for Current Active Safety Systems Using National Crash Databases. *Traffic Inj. Prev., 15*(7), 753–761. https://doi.org/10.1080/15389588.2013.871003
Lambert, B. (2018). *A Student's Guide to Bayesian Statistics*. SAGE Publications Ltd.
Land, M., & Horwood, J. (1995). Which parts of the road guide steering? *Nat., 377*(6547), 339–340. https://doi.org/10.1038/377339a0
Lappi, O., Pekkanen, J., Rinkkala, P., Tuhkanen, S., Tuononen, A., & Virtanen, J. P. (2020). Humans use optokinetic eye movements to track waypoints for steering. *Sci. Rep., 10*(1). https://doi.org/10.1038/s41598-020-60531-3
Lee, D. N. (1976). A theory of visual control of braking based on information about time-to-collision. *Percept., 5*(4), 437–459. https://doi.org/10.1068/p050437
Lee, H. C., Cameron, D., & Lee, A. H. (2003). Assessing the driving performance of older adult drivers: On-road versus simulated driving. *Accid. Anal. & Prev., 35*(5), 797–803. https://doi.org/10.1016/S0001-4575(02)00083-0
Lehtonen, E., Lappi, O., Koskiahde, N., Mansikka, T., Hietamäki, J., & Summala, H. (2018). Gaze doesn't always lead steering. *Accid. Anal. & Prev., 121*(August), 268–278. https://doi.org/10.1016/j.aap.2018.09.026
Li, A., Jiang, H., Zhou, J., & Zhou, X. (2019). Implementation of human-like driver model based on recurrent neural networks. *IEEE Access, 7*, 98094–98106. https://doi.org/10.1109/ACCESS.2019.2930873
Li, L., & Chen, J. (2010). Relative contributions of optic flow, bearing, and splay angle information to lane keeping. *J. of Vis., 10*(11), 1–14. https://doi.org/10.1167/10.11.16
Li, P., Merat, N., Zheng, Z., Markkula, G., Li, Y., & Wang, Y. (2018). Does cognitive distraction improve or degrade lane keeping performance? Analysis of time-to-line crossing safety margins. *Transp Res. Part F: Traffic Psychol. and Behav., 57*, 48–58. https://doi.org/10.1016/j.trf.2017.10.002
Lunn, D., Jackson, C., Best, N., Thomas, A., & Spiegelhalter, D. (2012). *The BUGS Book Bayesian Analysis*. Chapman & Hall / CRC Press.
Lynch, S.M., 2007. Introduction to Applied Bayesian Statistics and Estimation for Social Scientists. In Statistics for Social and Behavioral Sciences. Springer.
Macadam, C. C. (2003). Understanding and modeling the human driver. *Veh. Sys. Dyn., 40*(734), 101–134.
Makishita, H., & Matsunaga, K. (2008). Differences of drivers' reaction times according to age and mental workload. *Accid. Anal. & Prev., 40*(2), 567–575. https://doi.org/10.1016/j.aap.2007.08.012
Mammar, S., Glaser, S., & Netto, M. (2006). Time to line crossing for lane departure avoidance: a theoretical study and an experimental setting. *IEEE Trans. on Intell. Transp. Sys., 7*(2), 226–241. https://doi.org/10.1109/TITS.2006.874707
Markkula, G., 2015. Driver behavior models for evaluating automotive active safety: From neural dynamics to vehicle dynamics [Doctoral thesis, Chalmers University of Technology].
Markkula, G., Benderius, O., & Wahde, M. (2014). Comparing and validating models of driver steering behaviour in collision avoidance and vehicle stabilisation. *Veh. Sys. Dyn., 52*(12), 1658–1680. https://doi.org/10.1080/00423114.2014.954589
Markkula, G., Boer, E., Romano, R., & Merat, N. (2018). Sustained sensorimotor control as intermittent decisions about prediction errors: Computational framework and application to ground vehicle steering. *Biol. Cybern., 112*(3), 181–207. https://doi.org/10.1007/s00422-017-0743-9
Martínez-Garcia, M., Gordon, T., 2017. Human control of systems with fractional order dynamics. 2016 IEEE Int. Conf. on Sys., Man, and Cybern., SMC 2016 - Conf. Proc., 2866–2871. https://doi.org/10.1109/SMC.2016.7844674.
Martínez-García, M., & Gordon, T. (2017). A multiplicative human steering control model. *Proc. of the 2017 IEEE Int. Conf. on Sys., Man, and Cybern., SMC 2017*, 1–6. https://doi.org/10.1109/SMC.2017.8123158.
Martínez-García, M., Gordon, T., 2018. A New Model of Human Steering Using Far-Point Error Perception and Multiplicative Control. In: Proc. of the 2018 IEEE Int. Conf. on Sys., Man, and Cybern., SMC 2018, 1245–1250. https://doi.org/10.1109/SMC.2018.00218.
Martínez-García, M., Zhang, Y., & Gordon, T. (2016). Modeling lane keeping by a hybrid open-closed-loop pulse control scheme. *IEEE Trans. on Ind. Inform., 12*(6), 2256–2265. https://doi.org/10.1109/TII.2016.2619064
McLaughlin, S.B., Hankey, J.M., Klauer, S.G., Dingus, T.A., 2009. Contrubuting factors to run-off-road crashed and near-crashes. DOT HS 811 079. [Report].
Mircea, D., 2019. Steering feedback fidelity in driving simulators. [Master thesis, Delft University of Technology.].
Mole, C. D., Kountouriotis, G., Billington, J., & Wilkie, R. M. G. (2016). Optic flow speed modulates guidance level control: new insights into two-level steering. *J. Exp. Psychol.: Hum. Percept. Perform., 42*(11), 1818–1838. https://doi.org/10.1037/xhp0000256
Mole, C. D., Lappi, O., Giles, O., Markkula, G., Mars, F., & Wilkie, R. M. (2019). Getting back into the loop: the perceptual-motor determinants of successful transitions out of automated driving. *Hum. Factors: J. Hum. Factors Ergon. Soc., 61*(7), 1037–1065. https://doi.org/10.1177/0018720819829594
Najm, W. G., Smith, J. D., & Yanagisawa, M. (2007). *Pre-Crash Scenario Typology for Crash Avoidance Research* (p. 810 767.). Dot Hs [Report].
Narula, S. C. (1979). Orthogonal polynomial regression. *Int. Stat. Rev., 47*(1).
National Academies of Sciences, Engineering, and Medicine, 2011. Design of the In-Vehicle Driving Behavior and Crash Risk Study. The National Academies Press. https://doi.org/10.17226/14494.
Navarro, J., Deniel, J., Yousfi, E., Jallais, C., Bueno, M., & Fort, A. (2017). Influence of lane departure warnings onset and reliability on car drivers' behaviors. *Appl. Ergon., 59*, 123–131. https://doi.org/10.1016/j.apergo.2016.08.010
Okafuji, Y., Mole, C. D., Merat, N., Fukao, T., Yokokohji, Y., Inou, H., & Wilkie, R. M. G. (2018). Steering bends and changing lanes: the impact of optic flow and road edges on two point steering control. *J. Vis., 18*(9), 1–19. https://doi.org/10.1167/18.9.14
Page, Y., Fahrenkrog, F., Fiorentino, A., Gwehenberger, J., Helmer, T., Lindman, M., Op den Camp, O., van Rooij, L., Puch, S., Fränzle, M., Sander, U., Wimmer, P., 2015. A comprehensive and harmonized method for assessing the effectiveness of advanced driver assistance systems by virtual simulation. The 24th Int. Tech. Conf. on the Enhanc. Saf. of Veh. (ESV).
Reed-Jones, J. G., Trick, L. M., & Matthews, M. L. (2008). Testing assumptions implicit in the use of the 15-second rule as an early predictor of whether an in-vehicle device produces unacceptable levels of distraction. *Accid. Anal. Prev., 40*(2), 628–634.
Robertshaw, K. D., & Wilkie, R. M. (2008). Does gaze influence steering around a bend? *J. of Vis., 8*(4), 1–13. https://doi.org/10.1167/8.4.18
Salvucci, D. D. (2006). Modeling driver behavior in a cognitive architecture. *Hum. Factors, 48*(2), 362–380. https://doi.org/10.1518/001872006777724417
Salvucci, D. D., & Gray, R. (2004). A two-point visual control model of steering. *Percept., 33*(10), 1233–1248. https://doi.org/10.1068/p5343
Shams El Din, A. H., 2020. Statistical modelling of critical cut-ins for the evaluation of autonomous vehicles and advanced driver assistance systems [Master thesis, Chalmers University of Technology].
SmartEye. (n.d.). http://www.smarteye.se/.
Sosa, J., & Aristizabal, J. P. (2022). Some Developments in Bayesian Hierarchical Linear Regression Modeling. *Rev. Colomb. de Estad., 45*(2), 231–255. https://doi.org/10.15446/rce.v45n2.98988
Sternlund, S. (2017). The safety potential of lane departure warning systems—A descriptive real-world study of fatal lane departure passenger car crashes in Sweden. *Traffic Inj. Prev., 18*(S1), S18–S23. https://doi.org/10.1080/15389588.2017.1313413
Strandroth, J. (2015). Validation of a method to evaluate future impact of road safety interventions, a comparison between fatal passenger car crashes in Sweden 2000 and 2010. *Accid. Anal. & Prev., 76*, 133–140. https://doi.org/10.1016/j.aap.2015.01.001
Summala, H. (2007). Towards Understanding Motivational and Emotional Factors in Driver Behaviour: Comfort Through Satisficing. In P. C. Cacciabue (Ed.), *Modelling Driver Behaviour in Automotive Environments* (pp. 189–207). Springer.
Summala, H., Nieminen, T., & Punto, M. (1996). Maintaining lane position with peripheral vision during in-vehicle tasks. *Hum. Factors: The J. of the Hum. Factors and Ergon. Soc., 38*(3), 442–451. https://doi.org/10.1518/001872096778701944
Svärd, M., Markkula, G., Bärgman, J., & Victor, T. (2021). Computational modeling of driver pre-crash brake response, with and without off-road glances: Parameterization using real-world crashes and near-crashes. *Accid. Anal. & Prev., 163*, Article 106433. https://doi.org/10.1016/j.aap.2021.106433
Svärd, M., Markkula, G., Engström, J., Granum, F., & Bärgman, J. (2017). A quantitative driver model of pre-crash brake onset and control. *Proc. Hum. Fact. Ergon. Soc. Annu. Meet., 61*(1), 339–343. https://doi.org/10.1177/1541931213601565

Szydłowski, T., Surmiński, K., & Batory, D. (2021). Drivers' psychomotor reaction times tested with a test station method. *Appl. Sci. (Switz.), 11*(5), 1–11. https://doi.org/10.3390/app11052431

Tuhkanen, S., Pekkanen, J., Rinkkala, P., Mole, C., Wilkie, R. M., & Lappi, O. (2019). Humans use predictive gaze strategies to target waypoints for steering. *Sci. Rep., 9*(1), 1–18. https://doi.org/10.1038/s41598-019-44723-0

Ungoren, A. Y., & Peng, H. (2005). An adaptive lateral preview driver model. *Veh. Sys. Dyn., 43*(4), 245–259. https://doi.org/10.1080/00423110412331290419

Utriainen, R., Pollanen, M., & Liimatainen, H. (2020). The safety potential of lane keeping assistance and possible actions to improve the potential. *IEEE Trans. on Intell. Veh., 5*(4), 556–564. https://doi.org/10.1109/TIV.2020.2991962

van Winsum, W., Brookhuis, K. A., & de Waard, D. (2000). A comparison of different ways to approximate time-to-line crossing (TLC) during car driving. *Accid. Anal. & Prev., 32*(1), 47–56. https://doi.org/10.1016/S0001-4575(99)00048-2

Virginia Tech Transportation Institute. (2019). *SHRP2 Eyeglance Data Dictionary*.

Warren, R. (1982). Optical transformation during movement: Review of the optical concomitants of egomotion. *Report No. AFOSR-TR-82-1028*. [Report] https://doi.org/10.4324/9780203162545-11.

Wherry, R. J. (1931). A new formula for predicting the shrinkage of the coefficient of multiple correlation. *The Ann. of Math. Stat., 2*(4), 440–457.

Wilkie, R., & Wann, J. (2003). Controlling steering and judging heading: retinal flow, visual direction, and extraretinal information. *J. of Exp. Psychol.: Hum. Percept. and Perform., 29*(2), 363–378. https://doi.org/10.1037/0096-1523.29.2.363

Wolfe, B., Seppelt, B., Mehler, B., Reimer, B., & Rosenholtz, R. (2019). Rapid holistic perception and evasion of road hazards. *J. of Exp. Psychol.: Gener.*. https://doi.org/10.1037/xge0000665

Wynne, R. A., Beanland, V., & Salmon, P. M. (2019). Systematic review of driving simulator validation studies. *Saf. Sci., 117*, 138–151. https://doi.org/10.1016/j.ssci.2019.04.004

Yacoub, E., Harel, N., & Uğurbil, K. (2008). High-field fMRI unveils orientation columns in humans. *Proc. of the National Acad. of Sci. of the U.S.A., 105*(30), 10607–10612. https://doi.org/10.1073/pnas.0804110105

Zhou, X., Jiang, H., Li, A., & Ma, S. (2020). a new single point preview-based human-like driver model on urban curved roads. *IEEE Access, 8*, 107452–107464. https://doi.org/10.1109/ACCESS.2020.3001208

Zhu, H., Li, L., Jin, M., Li, H., & Song, J. (2013). Real-time yaw rate prediction based on a non-linear model and feedback compensation for vehicle dynamics control. *Proc. Inst. Mech. Eng., Part D: J. of Automob. Eng., 227*(10), 1431–1445. https://doi.org/10.1177/0954407013482070

Zulkepli, K. A., Rahman, M. A. A., Zamzuri, H., & Hamid, U. Z. A. (2018). Reducing the intrusive driving behaviour in lane departure avoidance system using machine learning approach. *IEEE Conf. on Intell. Transp. Sys., Proc., ITSC*, *2018-March*, 1–6. https://doi.org/10.1109/ITSC.2017.8317655.